604523

PHILCO
A SUBSIDIARY OF Ford Motor Company,
RESEARCH LABORATORIES

Secondary Publication No. U-2736
WO 2237

RRL-TDR-64-124

SECOND QUARTERLY TECHNICAL REPORT

AN INVESTIGATION AND DEVELOPMENT OF FILM PROTECTED - CONVECTIVELY COOLED NOZZLES

Prepared for: Air Force Rocket Propulsion Laboratory
Research and Technology Division
Air Force Systems Command
Edwards, California

Under Contract: AF 04(611)-9705

Prepared by: R. L. Mitchell
H. L. Moody
A. M. Saul
W. L. Smallwood

Approved by:
D. A. Carrison
Assistant Director
Electromechanics Laboratory

20 August 1964

ABSTRACT

Presented is a summary of the analytical and experimental effort during the second quarter of a one year contract to investigate and develop a film protected, convectively cooled nozzle for advanced solid rocket applications. The work performed included thermochemical analyses of the reactions encountered in the boundary layer between the injectant, the free stream, and the nozzle wall; heat transfer analyses on alumina particle radiation and convection heat transfer to the nozzle wall; fluid mechanics analysis of injection into a turbulent boundary layer with accelerating flow; cold flow laboratory experiments on injection into a turbulent boundary layer through discrete holes; and rocket motor tests of the cooling concept on the Philco Solid Propellant Simulator.

CONTENTS

ILLUSTRATIONS

ILLUSTRATIONS (Continued)

SECTION 1

INTRODUCTION

The emphasis in present and future propellants for solid rocket motors has been toward higher impulse. This can be accomplished by either reducing the molecular weight of the exhaust products, increasing the flame temperature, or both. Presently, flame temperatures of the order of 6500°F to 6800°F are being considered. Many tests have been conducted with propellants in this category and they have shown that this increase in temperature has produced major problems in thermal-structural integrity and surface regression, especially for long duration applications.

The investigations and results of contract AF 04(611)-8387, "Applied Research for Advanced Cooled Nozzles" showed that thermal protection concepts capable of containing these high energy corrosive propellants are limited. One concept which showed feasibility was the film protected, convection cooled nozzle. The purpose of the present contract is to obtain further analytical definition as well as experimental verification.

This report summarizes the work conducted at Philco Research Laboratories during the second quarter of the one year contract. In most areas work was a continuation of that reported in the First Quarterly Technical Report.[1] The thermochemical analysis of the reactions encountered in the boundary layer between the injectant, the free stream, and the nozzle wall was completed. Heat transfer analyses were performed on alumina particle radiation to the nozzle wall and convection heat transfer for the sub-scale and demonstration nozzle contours. Efforts continued on an analytical and experimental investigation of the fluid mechanic aspects of injection into turbulent boundary layers. Four rocket motor tests were conducted on sub-scale nozzles in which convection cooling and convection cooling with injection were evaluated with methane as the coolant/injectant.

The culmination of the various aspects of this investigation is to provide sufficient analytical and experimental background to allow one to design and optimized film protected-convectively cooled nozzle. However, as is indicated in the results of the work performed during the past quarter there are still several areas which require better understanding. These areas will receive concentrated effort during the remainder of the program.

SECTION 2

STUDY AND ANALYSIS

2.1 THERMOCHEMISTRY

As a continuation of the work reported in the First Quarterly Report[1], thermochemical analyses with carbon tetrachloride as an injectant were accomplished. Also included are the analyses of CCl_4 and CH_4 with alumina removed from the boundary layer.

Carbon tetrachloride is a liquid under ambient conditions, and its use as an injection fluid involves the problems of flow regulation and boiling. Nevertheless, at the temperatures of interest it decomposes endothermically to carbon and chlorine. The resultant chlorine should be relatively unreactive with the walls of the injection capillaries. Thus, like methane, and unstable carbon-based molecule is being added to the boundary layer. Unlike CCl_4, however, the hydrogen which results from the endothermic decomposition of methane is relatively reactive above 4000°F with respect to the graphite throat contour.

The enthalpies, in BTU/lb, of the free stream and the free stream plus various weight percentages of CCl_4 have been computed as a function of temperature and are shown in Figure 2-1. As discussed in the First Quarterly Report[1], three ratios of injection gas to combustion gas mass flow rates have been considered, 1:9, 1:1, and 9:1. The combustion product spectrum chosen is that from the 6720°F aluminized propellant system simulated in composition by the so-called "Hot Solid" composition.

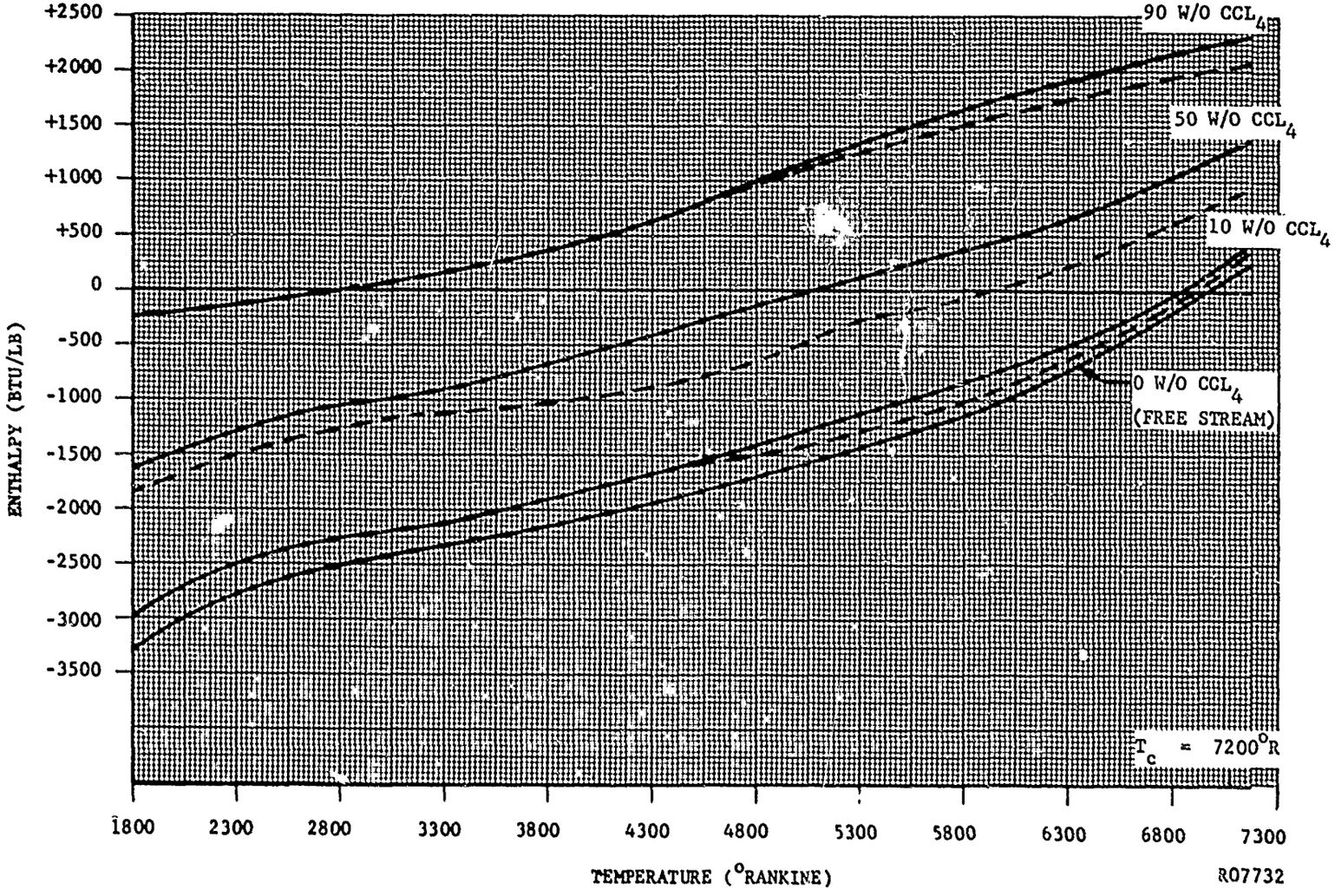

FIGURE 2-1. ENTHALPY VERSUS TEMPERATURE FOR EQUILIBRIUM MIXTURES OF "HOT-SOLID" - $CC1_4$ AT 400 PSIA

The enthalpy values shown represent the summation of the heat of formation at 536°R plus the change in enthalpy above that temperature of all of the combustion products and of the products of the reaction of the combustion products with CCl_4. These data, then, include the heats of any reactions which occur when CCl_4 is mixed with the free stream. Figure 2-1 also gives the enthalpy values if no chemical reactions between the CCl_4 and the combustion product species are allowed to occur. Assuming the enthalpy of mixing is zero, the difference in the enthalpy values at any given temperature with and without reaction represents the net heat of reaction at that temperature.

In comparing the enthalpy values of the CCl_4-free stream with those for CH_4-free stream given in the First Quarterly Report, it should be remembered that any direct comparison is on a mass basis, i.e., 10 pounds of CH_4 to 10 pounds of CCl_4. Since the injection capillaries represent a volume limited rather than a mass limited system, a truer comparison would be on a molar basis, i.e., the number of pound atoms of carbon being injected into the boundary layer per pound mole of injection gas. Thus, the 10 w/o CH_4 curves (10 lbs. CH_4 + 10 lbs combustion product gases) represent 10/16 or 0.62 lb moles of CH_4 and 0.62 lb atoms of carbon. 0.62 lb moles of CCl_4 (0.62 lb atoms of carbon) is represented by 92 lbs of CCl_4 and CH_4 is less exaggerated when compared on a molar basis rather than a mass basis.

The "B" values of CCl_4, i.e., the amount of wall material required to theoretically saturate one gram of the gas mixture (CCl_4 plus combustion products), are shown in Figure 2-2. A negative "B" value implies that there is more than sufficient carbon from the decomposition of the injectant carbon tetrachloride to saturate the mixture. As with the enthalpies, the 90 w/o CCl_4 curve can be compared directly to the 10 w/o CH_4 curve given in the first quarterly report. Again, the difference in the "B" values between CCl_4 and CH_4 is less exaggerated when compared on a molar basis rather than a mass basis. Indeed, when compared in this manner, CCl_4 offers a major advantage in that the Cl_2 is relatively inert to the graphite wall.

There is some question as to whether or not the condensed Al_2O_3 particles in the combustion free stream enter into the boundary layer. On this basis, calculations of enthalpies and "B" values have been made on mixtures of CCl_4-"Hot-Solid" and CH_4-"Hot-Solid," eliminating Al_2O_3 as a product of combustion, i.e., assuming that Al_2O_3 is neither reactive with the graphite wall nor the injection gas. The results are shown in Figures 2-3 through 2-6. As would be expected, the enthalpy values are more positive, reflecting the relatively high negative enthalpy of formation of Al_2O_3; and the "B" values are more negative, reflecting the reactivity of Al_2O_3 with the carbon in the boundary layer.

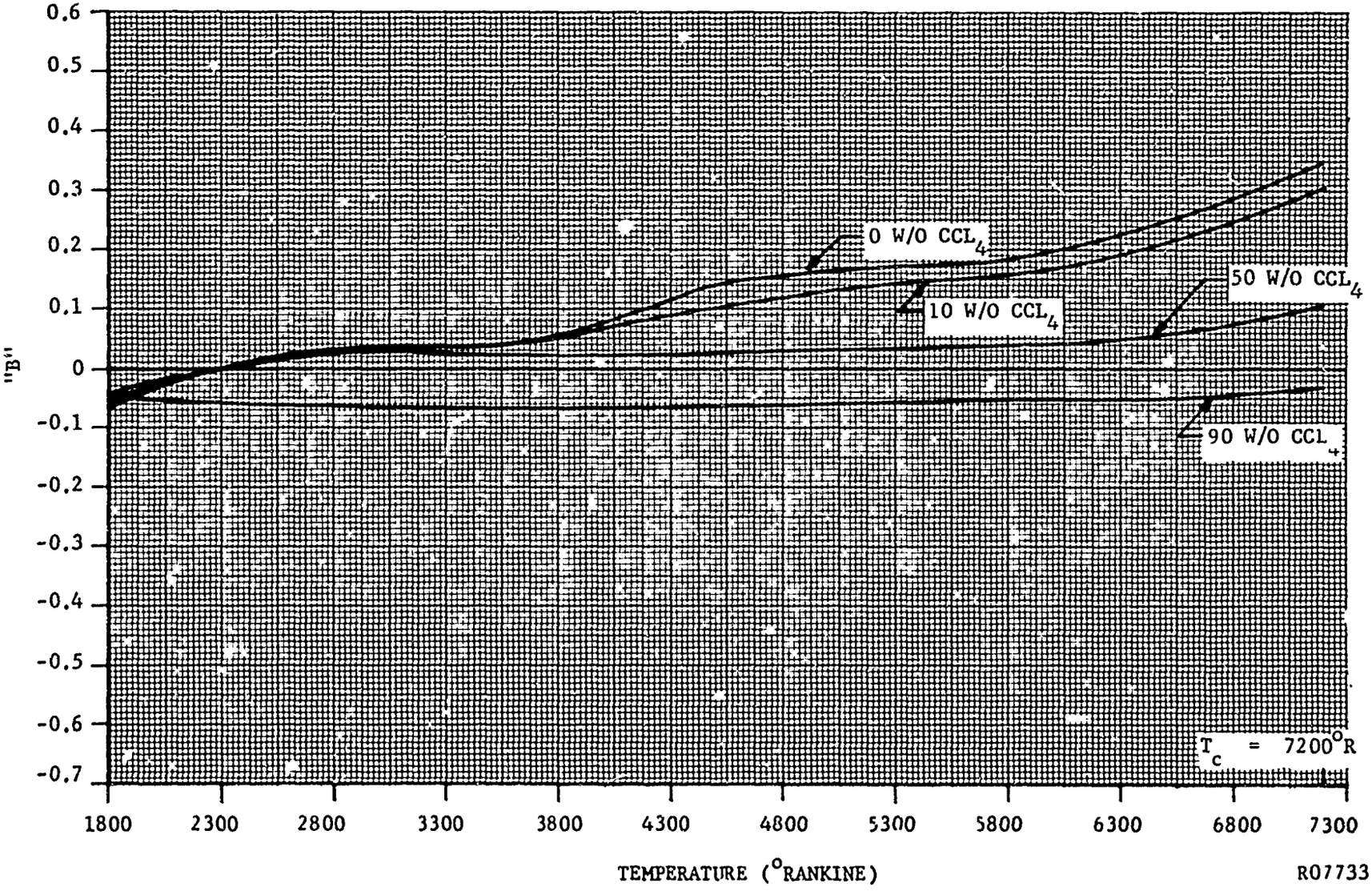

FIGURE 2-2 "B" VALUES FOR GRAPHITE IN EQUILIBRIUM WITH "HOT-SOLID" -CCl_4 MIXTURES AT 400 PSIA

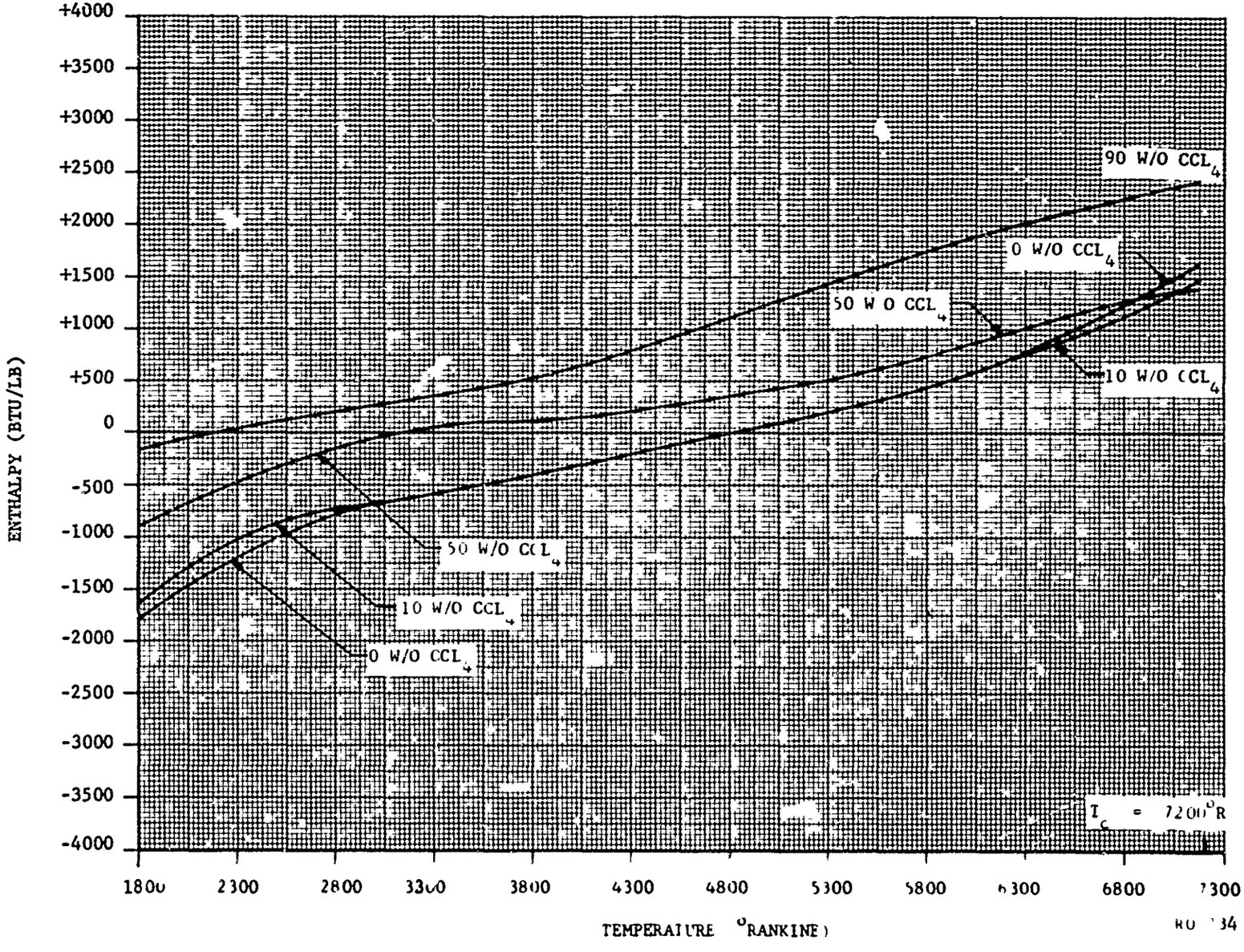

FIGURE 2-3. ENTHALPY VERSUS TEMPERATURE FOR EQUILIBRIUM MIXTURES OF "HOT-SOLID" - CCl_4 AT 400 PSIA ELIMINATING Al_2O_3 AS A PRODUCT OF COMBUSTION

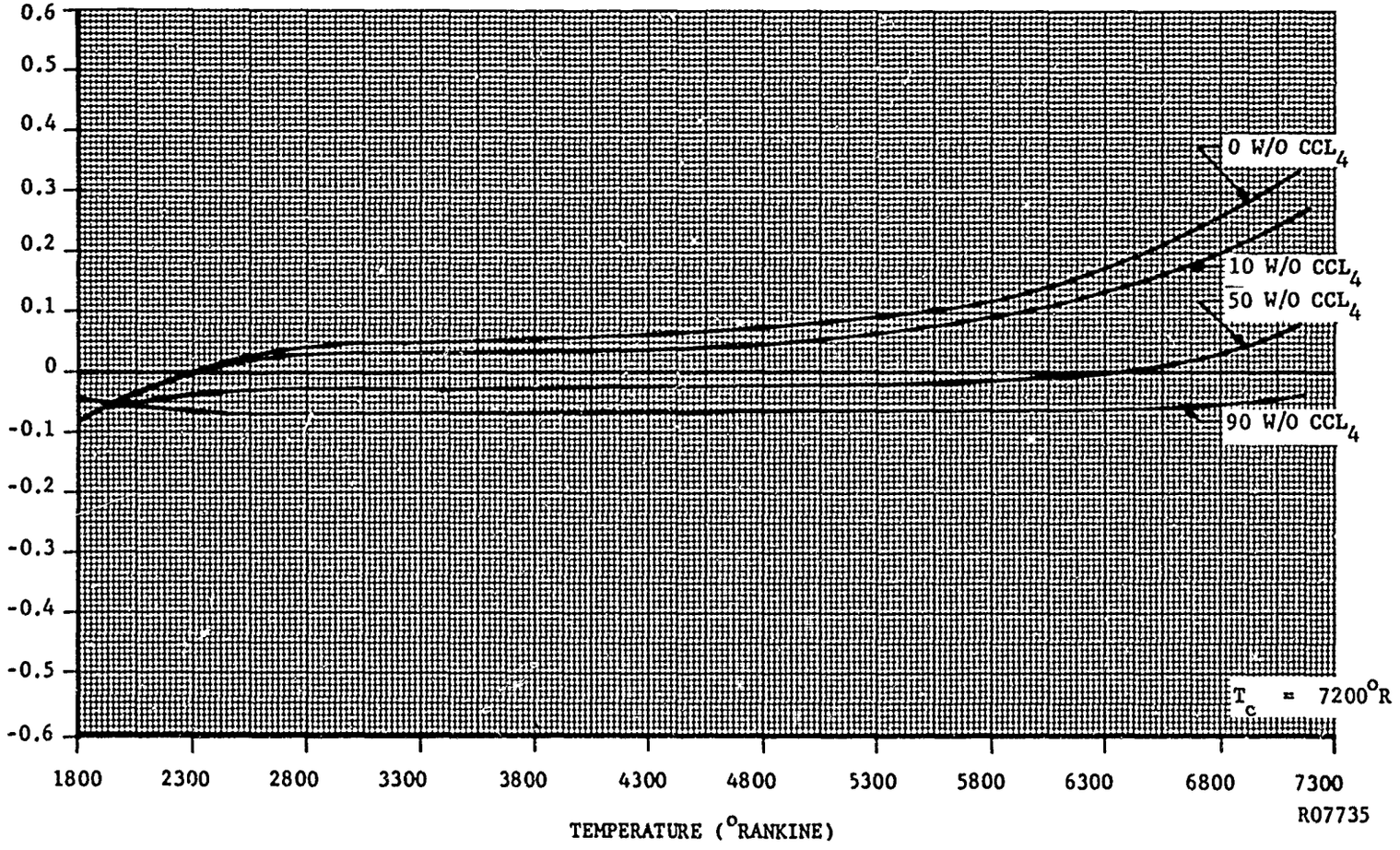

FIGURE 2-4. "B" VALUES FOR GRAPHITE IN EQUILIBRIUM WITH "HOT-SOLID"- CCl_4 MIXTURES AT 400 PSIA ELIMINATING Al_2O_3 AS A PRODUCT OF COMBUSTION

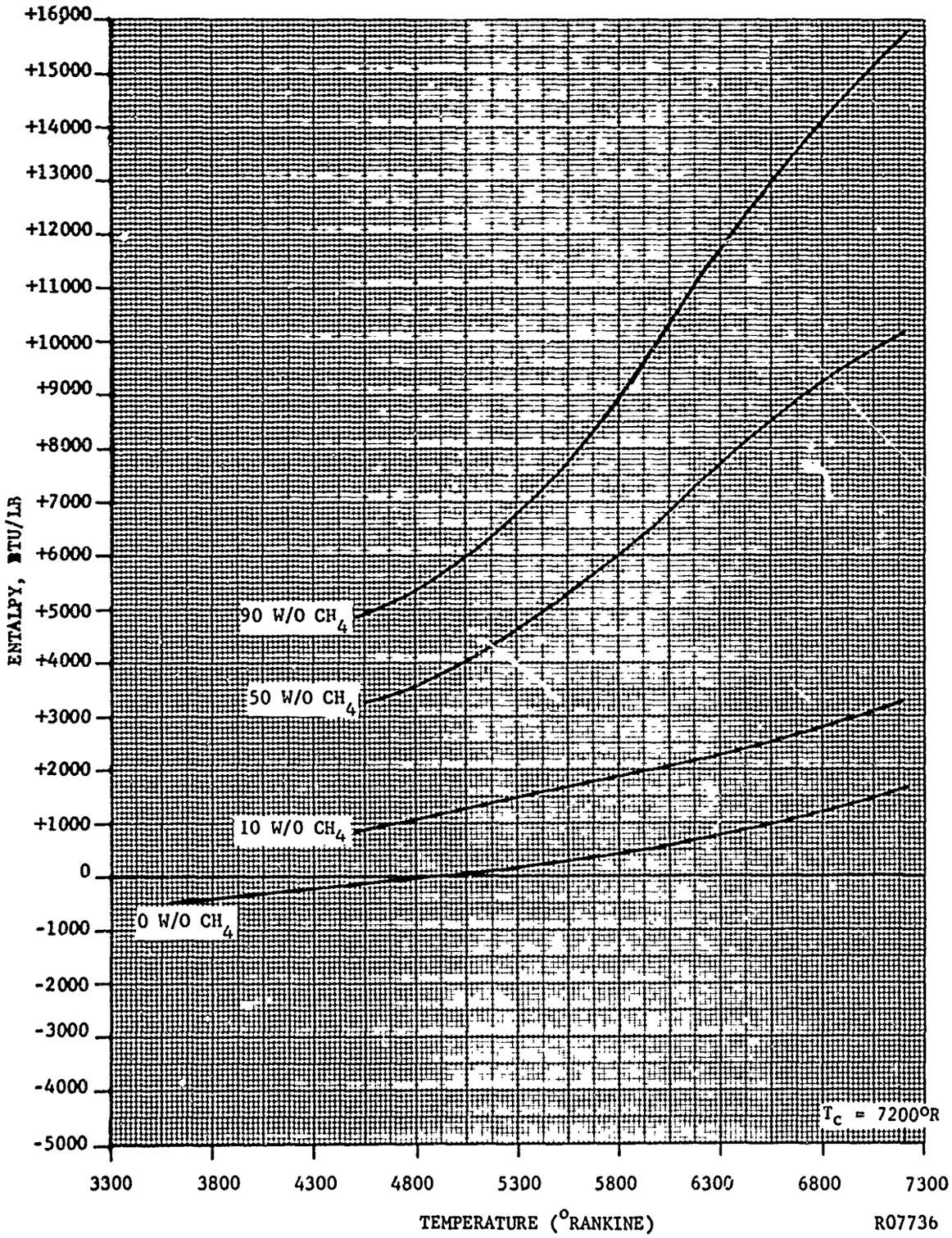

FIGURE 2-5. ENTHALPY VERSUS TEMPERATURE FOR EQUILIBRIUM MIXTURES OF "HOT-SOLID" - CH_4 AT 400 PSIA ELIMINATING Al_2O_3 AS A PRODUCT OF COMBUSTION

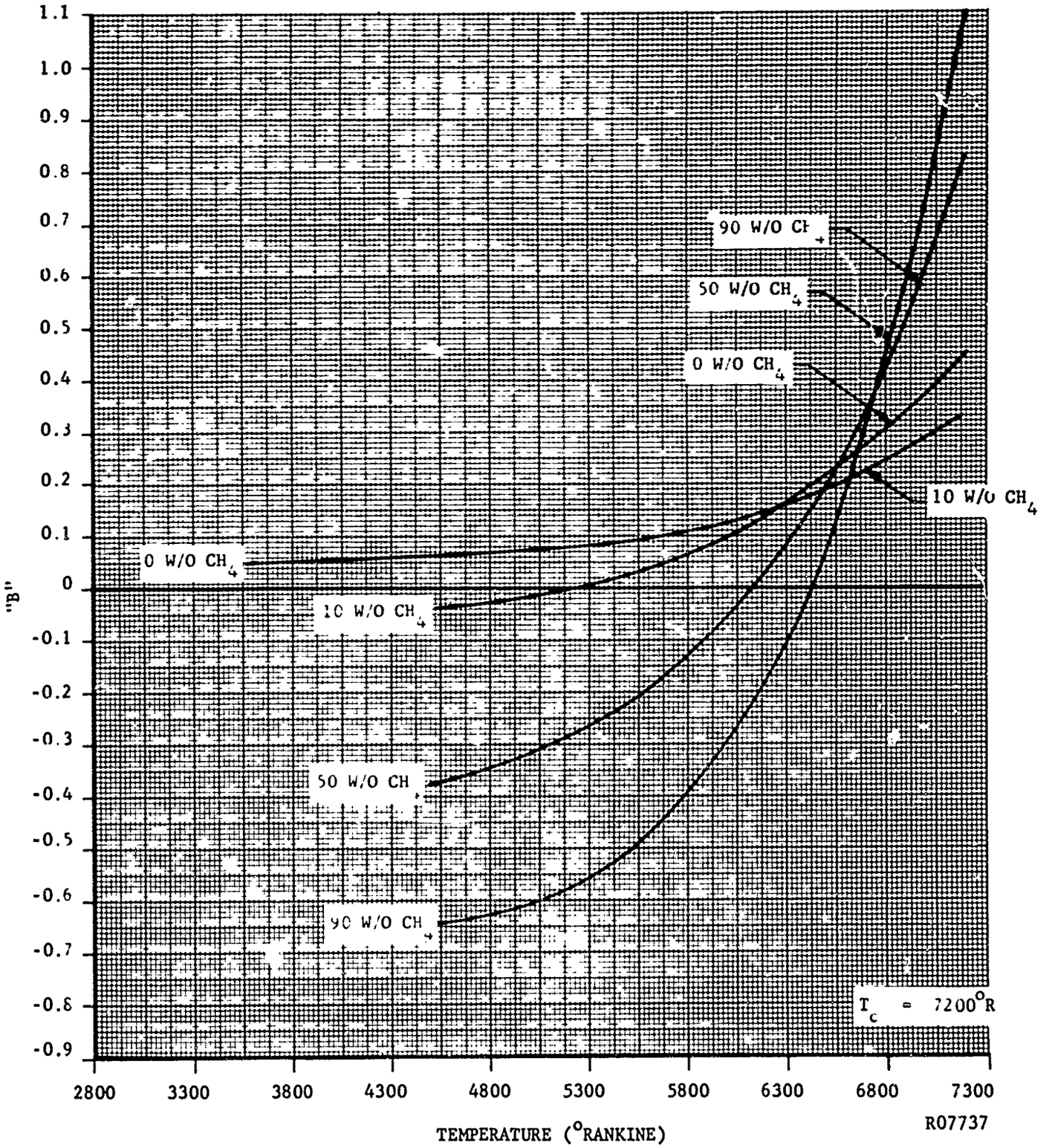

FIGURE 2-6. "B" VALUES FOR GRAPHITE IN EQUILIBRIUM WITH "HOT-SOLID" - CH_4 MIXTURES AT 400 PSIA ELIMINATING AL_2O_3 AS A PRODUCT OF COMBUSTION

2.2 FLUID MECHANICS

A primary advantage of the nozzle concept under study is that the opportunity of moderating the thermal and chemical action of the combustion products on the nozzle contour is provided through the use of controlled fluid injection. The objectives of the fluid mechanics studies have essentially been (1) to determine the nature of the interaction resulting when discrete three dimensional wall jets are injected into the boundary layer in the nozzle inlet and (2) to formulate an analytical model capable of predicting the thermal and chemical consequences of the fluid injection along the nozzle contour.

The cold flow injection studies covered in Section 3.1 are felt to have provided adequate insight into the problem of the injection interaction. However, considerable uncertainty remains concerning the formation of a two dimensional wall jet in a nozzle from a large number of three dimensional wall jets. Fortunately, there is no absolute reason why a uniform film need ever be achieved in the nozzle. The penalty for sacrificing the continuous film appears to be limited to a reduction in the effectiveness (thermal and chemical) of the fluid and the formation of slight irregularities on the contour. It is currently felt that actual nozzle firings will provide the only reliable indication of the occurance of jet coalescence. The fourth subscale test (with methane injection) is interesting in this regard. The apparent failure of the internal methane manifolds led to nonuniform injection. Additionally the pyrolytic graphite washer surface temperature, injection gas mixing and/or injection gas nonequilibrium effects were great enough to promote chemical reaction between the methane and graphite. The resulting grooves mark the extent of jet spreading. In some areas the jets actually coalesced in about 10 hole diameters. In other areas the jet patterns remained quite narrow and did not coalesce. It is thought that the wide patterns correspond to relatively low methane injection rates and the narrow patterns correspond to local injection rates which approached the design values. It is also felt that the major loss of material just upstream of the throat of this nozzle was due to a thermo-structural failure of the surface and was not a direct consequence of the fluid injection. However, the excessive surface temperatures implied here are due to inadequate cooling (or poor design heat transfer predictions) and could be related to the presence of the internal cooling passages near the surface. In comparison, the nitrogen injection nozzles tested during contract AF 04(611)-8387 were significantly cooler due to higher internal convection cooling capacity. These nozzles did not experience major contour failures upstream of the throat and uniform injection was apparently realized. The injection jet patterns were also observable in these tests because the surface under the core of the jet was completely protected from corrosion. The actual circumferential spreading of the inert jets is obscured somewhat because dilution of the combustion products with nitrogen can only reduce the rate of reaction. Thus, the jet boundaries are not sharply defined. The interesting observation

is that the effective core of the jets persists for a considerable distance downstream of injection. The axial length of the observed ridge and groove pattern is evidently proportional to the injection to free stream velocity ratio. At the present time, it appears reasonable to conclude that the rate of jet spreading, whether due to turbulent convection, simple diffusion or a combination of these, is slow relative to the axial transport. It is also apparent that the partial failure of the nozzle surface downstream of the injection point produces an unstable situation and must be avoided. The instability results from the use of counterflow cooling. That is, the thinning of the nozzle wall downstream of the injection point leads to higher local wall temperatures in the cooling passage and hence higher cooling rates and higher cooling gas bulk temperatures. Subsequently, the hotter gas becomes less effective in cooling the washers upstream of the point of contour failure. Finally, the injected gas has less film cooling capacity and the effective heating rate at the point of contour failure should increase. This may then lead to propagation of the fault in the contour in the upstream direction and the instability increases. In future testing efforts will be specifically directed toward increased convective cooling of the washers just upstream of the throat region. It is expected that the effects of both inert and methane gas injection will become more obvious when contour integrity is insured.

At the beginning of this contract it was recognized that there was no possibility of analytically describing the fluid mechanic development of a three dimensional wall jet in the nozzle. It was also recognized that existing analyses for two dimensional wall jets could not be realistically applied to the present problem. Consequently, efforts were directed toward the development of an improved analytic description of a two dimensional wall jet in an axisymmetric nozzle. Basically, the approach taken was to start with the case of incompressable flow without heat transfer, mass transfer or chemical reactions. It was postulated that the essence and practicality of the more complex cases (compressable flow, heat transfer, etc.) could be determined from the solution of the simplest model possible. Several analyses were developed for the incompressable case. These are currently being formalized for presentation in a subsequent report. Unfortunately, these analyses are of such complexity as to require numerical solution. Although the extension of each analysis, to include the omitted effects mentioned above, does not appear to be out of the question, the increase in complexity would be extremely severe. It would not be possible, considering the additional requirements for computer programming and program checkout, to achieve any numerical solutions within the contract period. It is also felt that it would be extremely difficult to evaluate the accuracy of the analysis because of the necessity of including a number of rather severe assumptions. Specifically, turbulent transport parameters would have to be provided. Although it would be of significant general interest to complete the analysis, the immediate requirements for extending both the qualitative and quantitative understanding of film development dictate a shift of emphasis to a less sophisticated approach.

At the close of the second quarter a new approach to the film analysis was formulated and work was started on its development. Basically, it is planned to select an existing film cooling analysis to characterize the thermal development of the film. This will amount to assuming that the energy transfer from the combustion products to the film is the same as it would be to the wall with no injection. The wall recovery temperature will then tend to rise exponentially with distance. This kind of approach depends heavily on knowing the heat transfer coefficient to a wall which would be at the local film temperature. Consequently, efforts to improve the heat transfer computer program (Section 2.3) have been accelerated. Some of the available film cooling analyses have shown rather good accuracy in experiments where molecular weight ratios differ from unity. Unfortunately, very little experimental data is available for the case of both accelerating flow and nonunity molecular weight ratio. Following the selection of a reasonably accurate film cooling model, a simplified mass transport equation will be superimposed and the two equations will be solved numerically stepwise through the nozzle. At the present time it is felt that a turbulent mass transport model should be assumed. A diffusion model will also be considered for comparison. The initial results of this effort are expected to be available during the third quarter. It is expected that subsequent sub-scale nozzle test results (thermocouple data) will provide a good check on the results of the film analysis when the revised film coefficients are used in the thermal analyzer program. The appearance of the nozzle throat surface will provide the only clues to the accuracy of the mass transport analysis.

2.3 HEAT TRANSFER

a. Flame Side Radiation

During the second quarter, some consideration was devoted to the evaluation of the radiant heat interchange between the walls and combustion products of the film protected nozzle. The radiation expressions presented in the first quarterly report were modified to include the effect of particle emission. Specifically, the equations representing the transmissivity and emissivity of a gas were no longer valid with the presence of a scattering media.

The scattering induced by the presence of alumina particles is sufficient to substantially alter the emission characteristics of an absorbing gas. For example, from References 2 and 3, the monochromatic emissivity of an isothermal homogeneous particle cloud may be expressed as:

$$\epsilon_\lambda = \frac{\gamma^a_{g\lambda} + \gamma^a_{p\lambda} + \gamma^{s1}_{p\lambda}}{\gamma^a_{g\lambda} + \gamma^a_{p\lambda} + \gamma^{s2}_{p\lambda}} \left[1 - e^{-\left(\gamma^a_{g\lambda} + \gamma^a_{p\lambda} + \gamma^{s2}_{p\lambda}\right)\ell}\right]$$

where γ^a is defined as the absorption coefficient, γ^{s1} is proportional to the energy scattered by a control volume in a specified direction and γ^{s2} represents the energy scattered by particles between 0 and ℓ (path length) that originates in the control volume. Recently, data has been acquired at Philco Research Laboratories on the monochromatic emissivity of molten alumina particles (Reference 2). The data was obtained from an alumina cloud that was optically thin and at temperatures approaching 5200°R. However, the condition of optical thinness will reduce the emissivity of a particle cloud to

$$\epsilon_\lambda = \gamma^a_{p\lambda}\,\ell$$

with γ^a_g set equal to zero (transparent gas). Applying the absorption coefficient, γ^a_p, found for the optically thin case to an optically thick medium will result in an unpredictable error in emission (e.g., unpredictable in the sense that the magnitude of scattering, which is entirely neglected, has not yet accurately been evaluated).

Assuming negligible scattering, the data of Reference 2 may be applied to cases below 5200°R. Above this temperature, extrapolation is required. Such extrapolation may induce major errors due to the potentially complicated dependency of alumina emissivity on temperature. Therefore, as was noted in Reference 3, the total emissivities obtained from the spectral emissivities of Reference 2 should only be applied to cases where approximate calculations suffice.

Calculations were made for the film protected nozzle utilizing the previously described total emissivities with the results presented in Figure 2-7. The radiant heat flux in the chamber is shown to be rather large relative

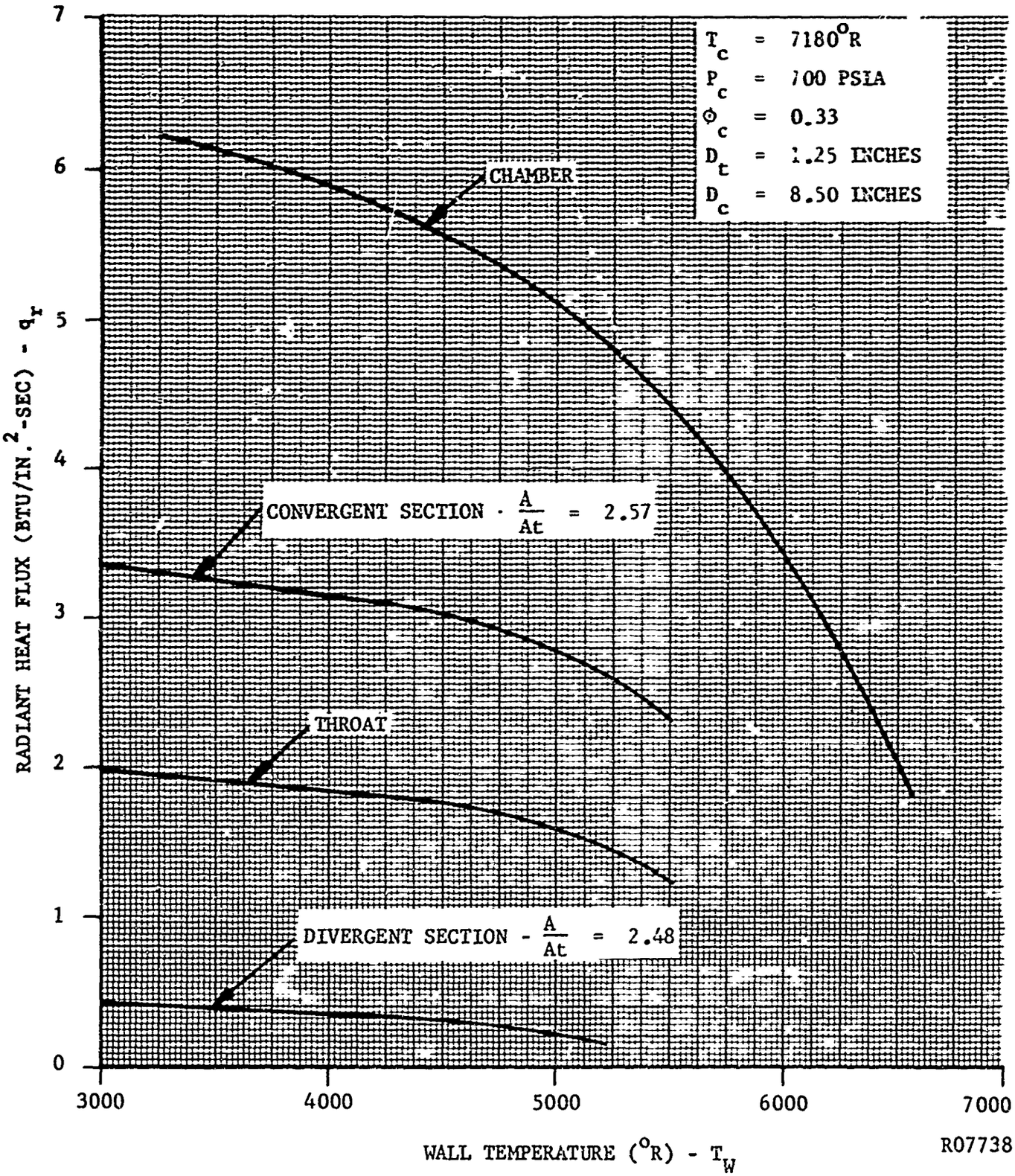

FIGURE 2-7. DEPENDENCE OF ALUMINA CLOUD RADIATION HEAT FLUX ON WALL TEMPERATURE FOR THE FILM PROTECTED NOZZLE

to previously predicted values. However, it must be remembered that the chamber is subjected to a large heat flux only during the transient heating period. At near steady state conditions the wall temperature is estimated at 4500°R with a heat flux of 2.0 Btu/in^2-sec. This value of heat flux, together with the others presented in Figure 2-7, are conservative but provide a reasonable estimate of the importance of alumina cloud radiation.

b. Flame Side Convection

During the second quarter, convective heat transfer coefficients were calculated for both the 1.25 and 2.50 inch throat diameter nozzle contours. The contours feature (1) 30 to 1 contraction and 10 to 1 expantion ratios, (2) 30° conical inlet, (3) 20° conical exit and (4) circular throat with a curvature to throat radius ratio of 2.0. The method of calculating the boundary layer growth and heat transfer coefficients is presented in Reference 4. Figure 2-8 is a plot of the convective heat flux calculated for the subscale nozzle (1.25 inch diameters throat). The alumina cloud radiation heat flux has been superimposed to show the total predicted heat flux. The data is presented in this manner to demonstrate both the apparent relative importance of alumina cloud radiation and the potential danger of basing the nozzle inlet thermal protection design solely on convective heat transfer predictions. It may be observed that the constant wall temperature cooling requirements increase from 127% of the convective flux, one inch upstream of the throat, to 280% three inches upstream. This is precisely the region where major inlet failures have occurred in testing during the present contract and during contract AF 04 (611)-8387 as well. It should also be noted that the fluid injection will not be as effective in reducing or controlling the wall temperatures in the inlet region when radiation is the primary mode of heat transfer. This situation also provides a qualitative explanation for the observed corrosivity of the injected methane during the fourth subscale nozzle test.

During the third quarter, the heat transfer coefficients used by the thermal analyzer computer program will be changed to include the revised estimates of the radiation contribution to the total heat transfer. It is anticipated that the results will indicate that some design changes will be required in order to insure adequate thermal protection of the nozzle inlet. Also, to achieve greater insight into the accuracy of the radiation analysis, an effort will be made to obtain transient temperature histories for the simulator's graphite chamber liner. Since the convective heat transfer to the liner is about an order of magnitude less than the radiative contribution, it should be reasonably easy to distinguish the presence of large radiation heat fluxes. In the interim, nozzle testing will proceed using cooling gas mass flow rates which will be 25 to 50% higher than the original estimates in order to improve inlet performance. If this step is not taken, it would appear that the value of the film injection will be extremely difficult to evaluate because the

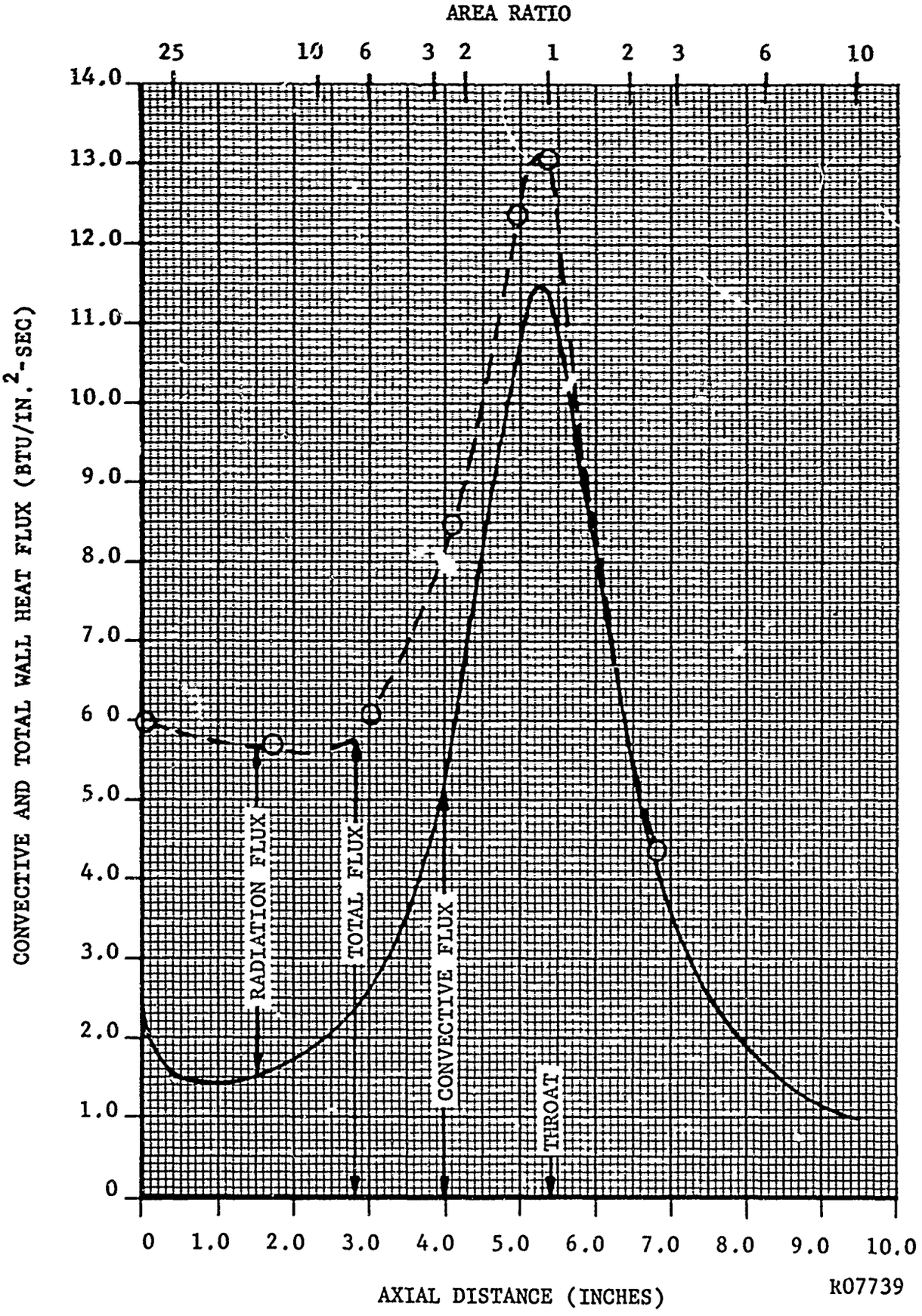

FIGURE 2-8. CONVECTIVE AND TOTAL HEAT FLUX FOR AN ISOTHERMAL NOZZLE WALL

failure of the inlet contour will lead to nonuniform injection and eventually to failure of the cooling passage walls.

In the first quarterly report, it was suggested that the boundary layer heat transfer program (Reference 4) could be used to estimate the change in heat transfer due to the film injection. Several trial calculations were made in which the boundary layer energy thickness was arbitrarily increased by as much as a factor of two at the point of injection while the momentum thickness was not changed. The changes in energy thickness were chosen to correspond roughly to the additional energy deficit which would result from the injection of a continuous film of methane at the preliminary design flow rate. The calculations showed less than a 10% reduction in the throat heat transfer coefficient when free stream transport properties were used. This was found to be primarily due to a combination of the use of a logarithmic skin friction law in the computer program and the fact that the energy thic ness Reynold's number was very large at the injection point. From this it follows that the heat transfer coefficient would be more sensitive to the value of the boundary layer specific heat than to the energy thickness. Therefore, the addition of hydrogen (from the methane dissociation) could lead to increased in the heat transfer roughly proportional to the degree to which the injection gases mix with the free stream and to the difference in specific heats of the two gas streams. Since this type of model apparently obscures the important mixing and film cooling effects which are known to exist, it can not be regarded as a particularly useful mechanical means of investigating film injection.

As indicated in the first quarterly report, the boundary layer program (Reference 4) is also being examined to delineate changes which could improve both the theory and programming. One such improvement would be to remove the restriction of the use of the 1/7th power law velocity and temperature profile assumption which is used to determine the boundary layer shape parameters. At the high Reynold's numbers which pertain to the present problem, higher order profiles should be used. A method for determining the appropriate value of the power law exponent is available and could be used. Another area of interest is the one dimensional flow assumption. Currently, a method of calculating the axisymmetric flow conditions at the edge of the boundary layer is being examined. This method would utilize the transonic flow analysis by Hall, Reference 5, and the axisymmetric version of the nozzle flow analysis described by Holt, Reference 6. It is also apparently desirable to minimize the use of the perfect gas law assumption in the program. The use of variable free stream properties can be incorporated by using the results of the rocket propellant performance program with the present heat transfer program. It is expected that some of these changes will be made and further evaluated under another contract. However, during the third quarter, efforts in the area of flame side heat transfer will be confined to the evaluation of the radiation heat transfer and to the investigation of potential film cooling effects.

SECTION 3

LABORATORY EXPERIMENTS

3.1 COLD FLOW TESTS

During the second quarter, the cold flow testing has been devoted to the evaluation of the fluid mechanic properties of parallel three dimensional wall jets. The present testing was, essentially, a continuation of the injection studies presented in Reference 1 with concentration in the area of wall coverage. The important parameters that were studied which effect wall coverage by a protective wall jet consisted of hole spacing, injection rate, injection angle, and hole size.

The cold flow injection apparatus used in the first quarter was slightly altered in that the tubular wall was lined with ozalid paper and ammonia was employed as the injectant. By injecting ammonia into a nitrogen main stream in the form of a wall jet, the concentration of ammonia at the wall can distinctly be determined from reaction zones developed on the downstream ozalid paper, the degree of the ammonia - ozalid paper reaction being a function of ammonia concentration.

A technique had to be developed in the ozalid tests in order to (1) reproduce identical flow conditions that existed in Reference 1 and (2) obtain reproducible data between experiments. In order to reproduce flow conditions, the Pitot probe and tubular end support section were assembled in the exact configuration that existed in Reference 1 after lining the wall with ozalid paper. Since the degree of the ammonia - ozalid paper reaction is sensitive to temperature, infrared radiation, time of exposure to ammonia, and ammonia concentration, it is important that each run be subjected to identical developing techniques. Therefore, in each run the ammonia exposure time was fixed at 5 minutes and the

experiment was run without exposure to sunlight. With the more important developing variables fixed, doubts remained concerning the problem of ozalid paper developing and the results have been only considered qualitatively.

In the experiments, six different injection geometries were studied, all of which are listed in Table 3-1. In all cases the injection hole diameter was fixed at .0625". The injection angle is viewed from a plane passing through the axis of the tube and the injection point; whereas the skew angle is viewed on a plane normal to the axis of the tube.

TABLE 3-1

GEOMETRICAL CONFIGURATION OF INJECTION TEST PIECES

Injector	Injection Angle (degrees)	Skew Angle (degrees)	Hole Spacing (Diameters)
1	15	0	5-4-3-2.5-2
2	20	0	"
3	25	0	"
4	20	10	"
5	20	20	"
6	20	0	3-3-3-3-3

With each of the six injectors, three injection mass flow rates were run. These mass flows being representative of the $\rho u/(\rho u)_\infty$ and $\rho u^2/(\rho u^2)_\infty$ range expected in the actual nozzle. For fully developed turbulent pipe flow the velocity (u_∞) was taken at a height from the wall equal to the radius of the injection hole (Reference 1).

Under the flow conditions that existed in the injection tests no measurable difference in wall coverage was experienced at injection angles of 15, 20 and 25° and skew angles of 10 and 20°. Figure 3-1 is, therefore, representative of the injection tests utilizing test pieces 1 through 5. Figure 3-1 clearly indicates the longitudinal dependence of jet coalescence on hole spacing. The interaction of two parallel jets with the free stream induces a flow field in which ammonia transport is promoted in the circumferential direction a few hole diameters downstream of injection.

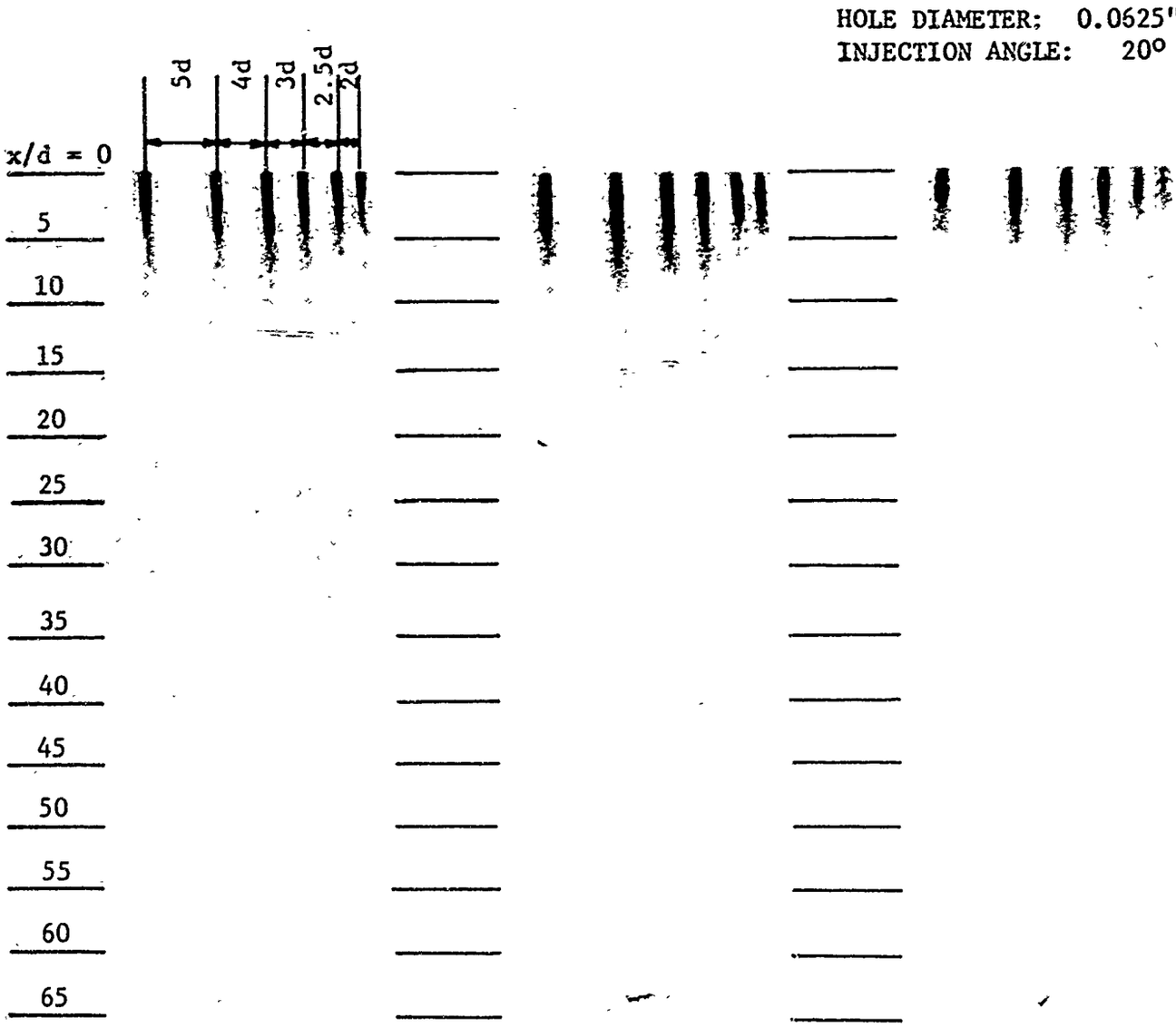

R07740

FIGURE 3-1. WALL COVERAGE BY FILM INJECTION WITH VARIABLE HOLE SPACING

In the region of coalescence there exists certain distinct areas of jet mixing. The first is near the injection point, where there is a large concentration of ammonia which is defined by the dark core of the jet. In this region, the main stream is not yet mixed with the jet and the presence of the core seems to exist as far as five diameters downstream. Beyond that, the core has mixed with the free stream and uniform wall coverage is achieved for hole spacings as large as three diameters. In this area the wall jet may be said to have lost its three dimensional character and the assumption of a two dimensional wall jet is applicable. The transition of a three to a two dimensional wall jet was also observed from a circumferentially ρu^2 traverse. Downstream of coalescence the wall concentration of ammonia decreases due to mixing with the main stream. The wall jet is preserved further downstream for closer hole spacings. This can be expected due to the greater amount of mass injection per unit circumferential length.

The dependence of wall coverage by a jet on the free stream velocity profile was determined by inserting a sandpaper trip just upstream of injection. The ρu^2 profiles with and without the sandpaper trip are shown in Figure 3-2. In both cases the ρu^2 traverses were made without injection and at the point of injection. Wall jet coverage with and without the trip is shown in Figures 3-3 and 3-4, respectively. The large decrease in downstream wall coverage in Figure 3-3 as compared to Figure 3-4 can be at attributed to the increase in main stream turbulence and to a greater free stream momentum flux acting upon the jet. Just downstream from injection the region between injection holes is slightly covered with NH_3. Whereas, for the case with fully developed turbulent pipe flow there are discrete regions where ammonia does not exist.

In photographing the injection results, the distinct color contrast that existed in the original ozalid paper is lost. Some of the interpretations presented above depend on the observation of the color contrast. Also, the puncture in the paper at about 60 diameters downstream of injection resulted from the assembling of the Pitot tube support system.

At the present time it is felt that the cold flow tests stand completed. The cold flow testing has added to and improved existing knowledge on detachment, velocity development and wall coverage of a three dimensional wall jet.

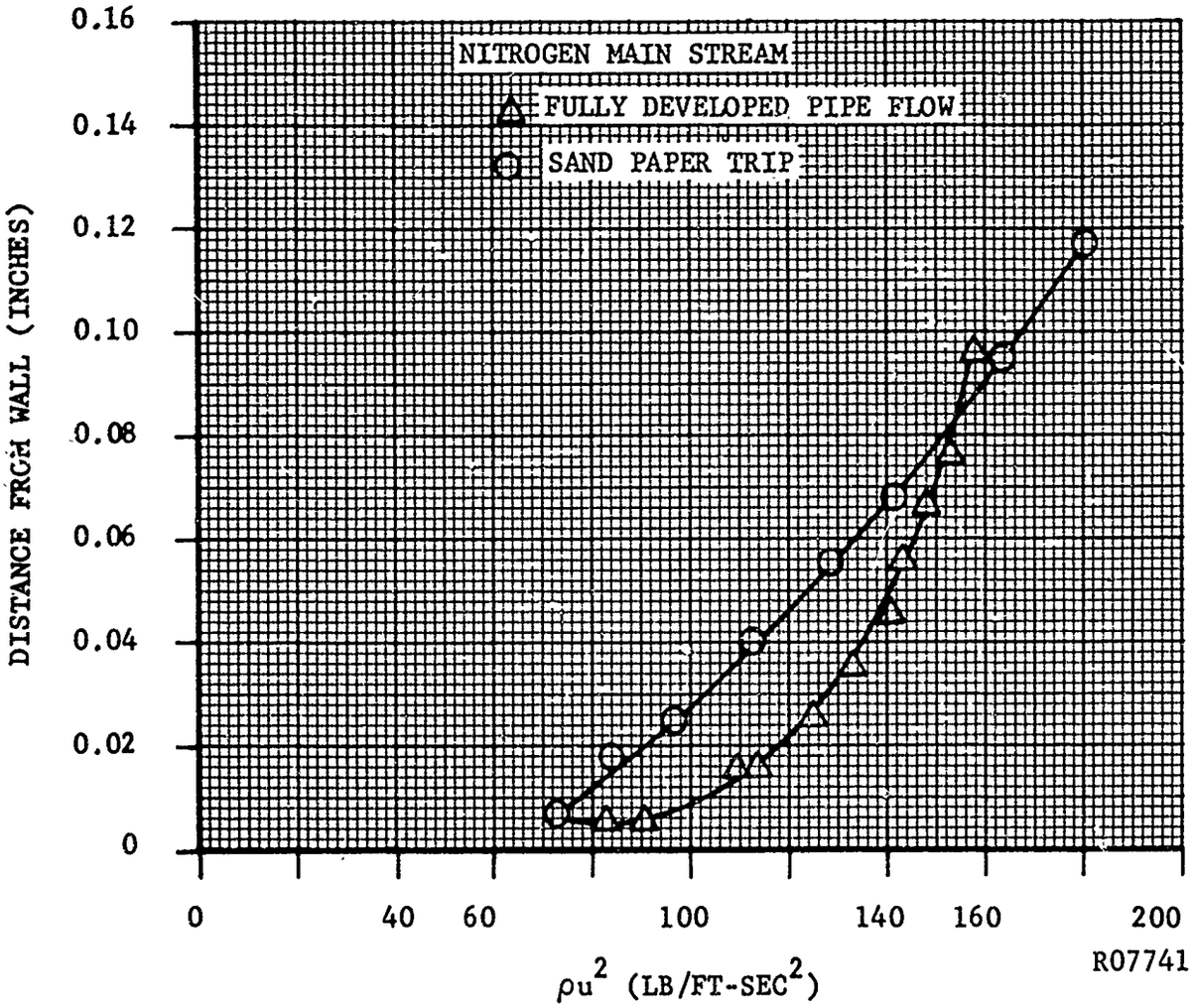

FIGURE 3-2. FREE STREAM PU^2 PROFILE AT LOCATION OF INJECTION HOLE WITHOUT MASS TRANSFER

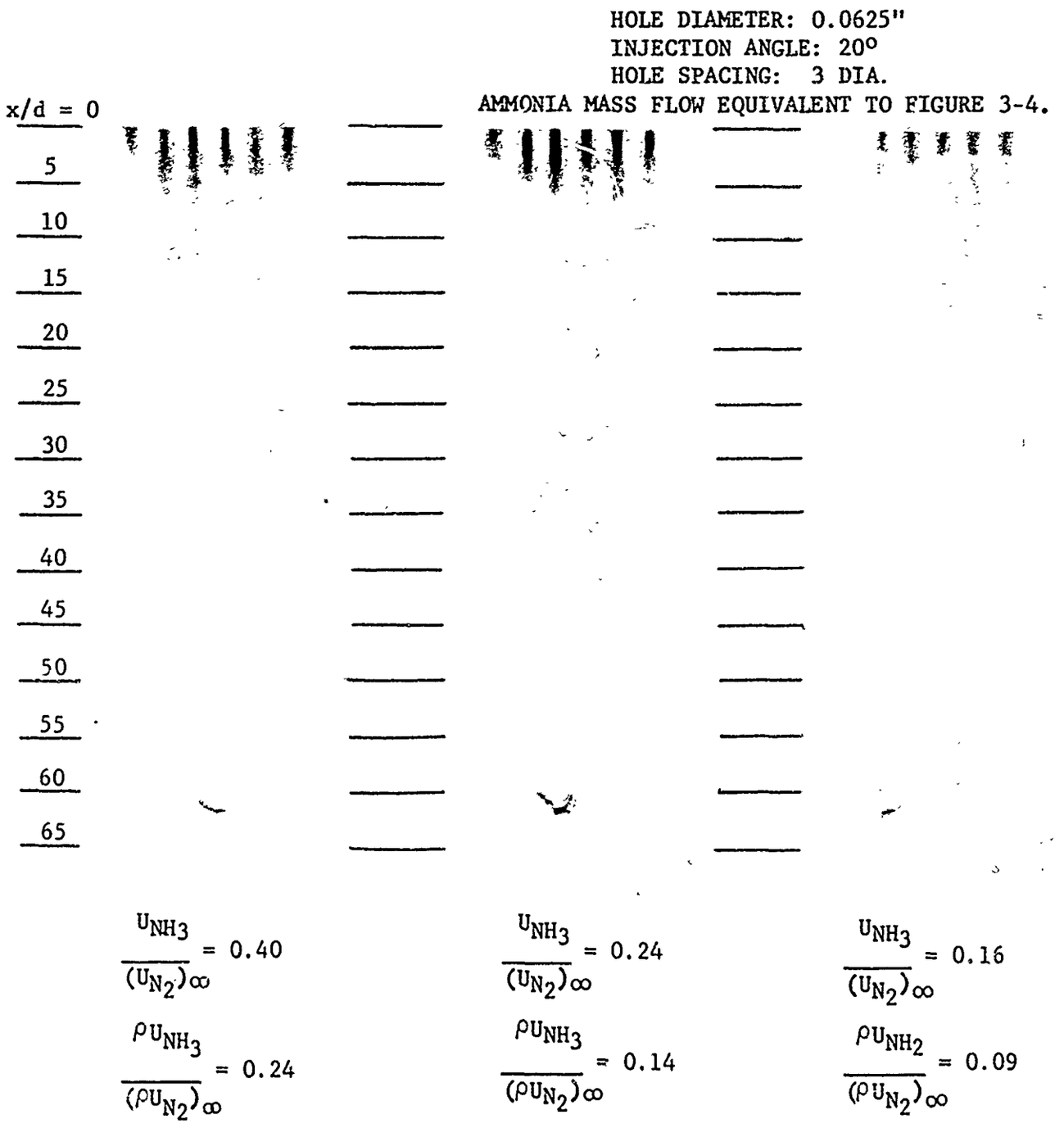

FIGURE 3-3. WALL COVERAGE BY FILM INJECTION WITH SANDPAPER TRIP

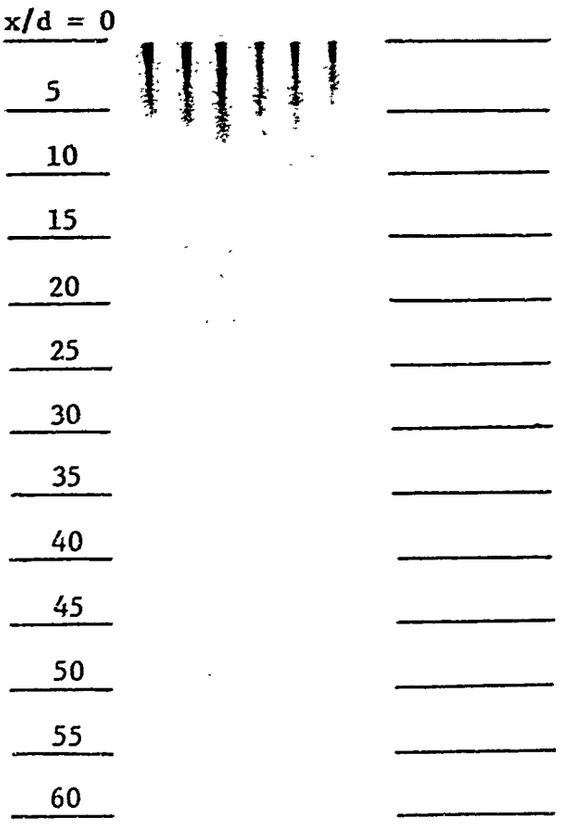

FIGURE 3-4. WALL COVERAGE BY FILM INJECTION WITH FULLY DEVELOPED TURBULENT PIPE FLOW

3.2 CONCLUSIONS

Wall coverage by a three dimensional jet was found to be independent of injection angle in the range studied. Injection angles of 15, 20, and 25 degrees were tested and within the accuracy of the experiment no measurable alteration of wall coverage was noted. Also, skew angles of 10 and 20 degrees resulted in no definite alteration of the flow field.

Wall coverage was found to be extremely dependent on hole spacing. Hole spacings larger than 5 diameters under the flow conditions existing in the cold flow tests are inadvisable as is shown in Figure 3-1. However, alteration of the free stream velocity boundary layer has shown to change the circumferential mass transport of ammonia (Figure 3-3).

An increase in the turbulence and velocity gradient of the main stream by tripping the existing fully developed turbulent pipe flow resulted in greater mixing near the injection point and a substantial reduction in downstream wall coverage. This is shown by a comparison of Figures 3-3 and 3-4. The application of a two dimensional analytical model to discrete hole injection is valid provided the hole spacing does not exceed approximately four diameters. Under the flow conditions that existed, a two dimensional wall jet was obtained at approximately five diameters downstream with a hole spacing of three diameters. Therefore, the assumption of a two dimensional model in an analytical interpretation of the problem is feasible within certain limits of hole spacing and free stream turbulence.

In the first quarter of the contract period a study of a three dimensional wall jet was made in areas of jet detachment and ρu^2 variation in the axial and circumferential directions. Jet detachment was found to be a function of momentum rate with the critical ratio of jet radial momentum rate ($\rho u\, u_r$) to free stream momentum rate ($\rho u^2)_\infty$ measured at approximately 0.4. A theoretical model was devised in which the critical ratio was evaluated at 0.6. Therefore, to avoid undesirable jet detachment, the momentum rate ratio should be kept below 0.4.

Radial ρu^2 traverses were made through a three dimensional wall jet at various downstream locations. These traverses were made for both the attached and detached wall jet. For the detached jet the ρu^2 profile may be divided into essentially three regions. The first being near the wall in which the free stream flows around the detached jet forming a separated region where a high degree of vorticity exists, similar to flow around a cylinder. The second region consists of the jet itself and the third is composed of the free stream. Between the three regions there exists

areas of large momentum transfer and therefore the profiles will change rapidly in the axial direction. For the attached jet, radial profiles resulted in termination of the mixing region at approximately 13 diameters downstream of injection. The ρu^2 profiles for the attached and detached jet are presented in the first quarterly report, pages 85 to 90.

The cold flow tests have produced good qualitative conclusions in areas of chemical protection by mass injection. Direct application of the results to an actual rocket nozzle is inadvisable although general knowledge on the properties or behavior of jets may be applied rather well.

SECTION 4

ROCKET MOTOR TESTS

4.1 CHEMICAL DIFFUSION TESTS

In the First Quarterly Progress Report the theory and preliminary design for the chemical diffusion motor tests were discussed. Early in the second quarter a series of four tests were run with completely unsatisfactory results. In the first test, an orifice sizing error led to a near stoichiometric mixture ratio in the H_2-O_2 generator. The resultant high temperature flame caused the copper nozzle to fail early in the test. The second test was run fuel rich for 45 seconds. The thermocouple readings indicated that the copper sleeve reached temperatures well above those required for oxidation. However, there was essentially no difference between the temperatures measured in line with the methane injection and those in an uncooled section of the copper sleeve. Close examination of the combustion chamber and copper sleeve indicated a rather severe helical swirl which accounts for the similarity in the temperature readouts. Additionally, no distinct oxidation pattern could be observed on the copper surface, presumably due to the reducing nature of the fuel rich flame. Both the third and fourth tests were run with an oxygen rich flame. In one test the nozzle and copper sleeve melted and in the other the stainless steel chamber ignited. It was concluded that oxygen rich operation at relatively low temperatures (1800-2000^{o}F) presented injector and flow control requirements that were too exacting for this simple experiment.

Several steps could be taken to improve the performance of the chemical diffusion motor. The addition of a mixing chamber and maintaining balanced methane injection would probably eliminate the injector swirl problems. The H_2-O_2 motor could be operated oxygen rich with an inert gas, such as nitrogen, added to control the flame temperature. It would also be possible to plate the copper detector sleeve with boron and run the motor

fuel rich. In this case the water-boron reaction would occur on those portions of the surface which were not protected by the film injection.

Action in the directions outlined above was temporarily suspended early in the second quarter pending the achievement of an improved injection film development model and several successful subscale motor firings. At the present time it is not clear just how the experiments as originally designed could be of use in support of the film analysis or nozzle test programs. Until a better definition of the essential objectives of this type of experiment is achieved, the continuation of the chemical diffusion tests will be de-emphasized. It is anticipated, however, that some experimental effort should eventually be undertaken to evaluate the integrity of the final film cooling-mass transport model of film development discussed in Section 2.2. During the third quarter the behavior of a boron plated copper plate, exposed to high temperature water vapor, will be examined in the laboratory employing the same technique previously used with the $Cu-O_2$ and $Ni-O_2$ systems.

4.2 SIMULATOR TESTS (SUB-SCALE)

During the second quarter of the contract period four nozzles were tested on the Philco Solid Propellant Simulator. The nominal test conditions were 1270 pounds thrust, 700 psia chamber pressure and 6700°F combustion temperature with a propellant containing 16% aluminum.

Tests 1 and 2 involved convection cooling of a pyrolytic graphite washer-type heat sink nozzle with methane. Tests 3 and 4 involved film injection of the methane into the entrance section after it had passed through the convection passages. The results of these tests are presented in the following paragraphs.

a. Nozzle Test No. 1

(1) Design Description

The configuration of the first nozzle tested is shown in Figure 4-1. The concept for this nozzle was to convectively cool a pyrolytic graphite washer-type heat sink with methane, then dump it overboard. It was the purpose to determine the effectiveness of temperature control on corrosion reduction.

The heat sink outside diameter was 5.0 inches and had a throat diameter of 1.25 inches. The convection passages were nominally 0.25 inches from the nozzle wall. There were 28 passages equally spaced and their diameter was 0.040 inches except in the throat washer where it was 0.030 inches.

The design methane flow rate was 0.001 lb/sec per passage or a total of 0.028 lb/sec. The calculated temperature distributions using the Thermal Analyzer Computer Program (Reference 1) is shown in Figure 4-2 along with the measured temperatures at the throat. The cooling analysis was based on the undissociated properties of methane.

(2) Test Results

The nozzle was run for 21.5 seconds at the conditions shown in Table 4.1. The chamber pressure vs. time is shown in Figure 4-3 and temperature histories are shown in Figure 4-4. Thermocouples used were the chromel-alumel type. Comparison of temperature measurements made in throat washer with analytical predictions are shown in Figure 4-2. The comparison of T_1 and T_5 (see location sketch in Figure 4-4) is given in Table 4.2.

As is indicated by chamber pressure there was no measurable corrosion. Inspection of the nozzle after the test showed no corrosion at any point in the entrance or exit section. This should be expected since the wall temperature at no point in the nozzle should be greater than 5000°F.

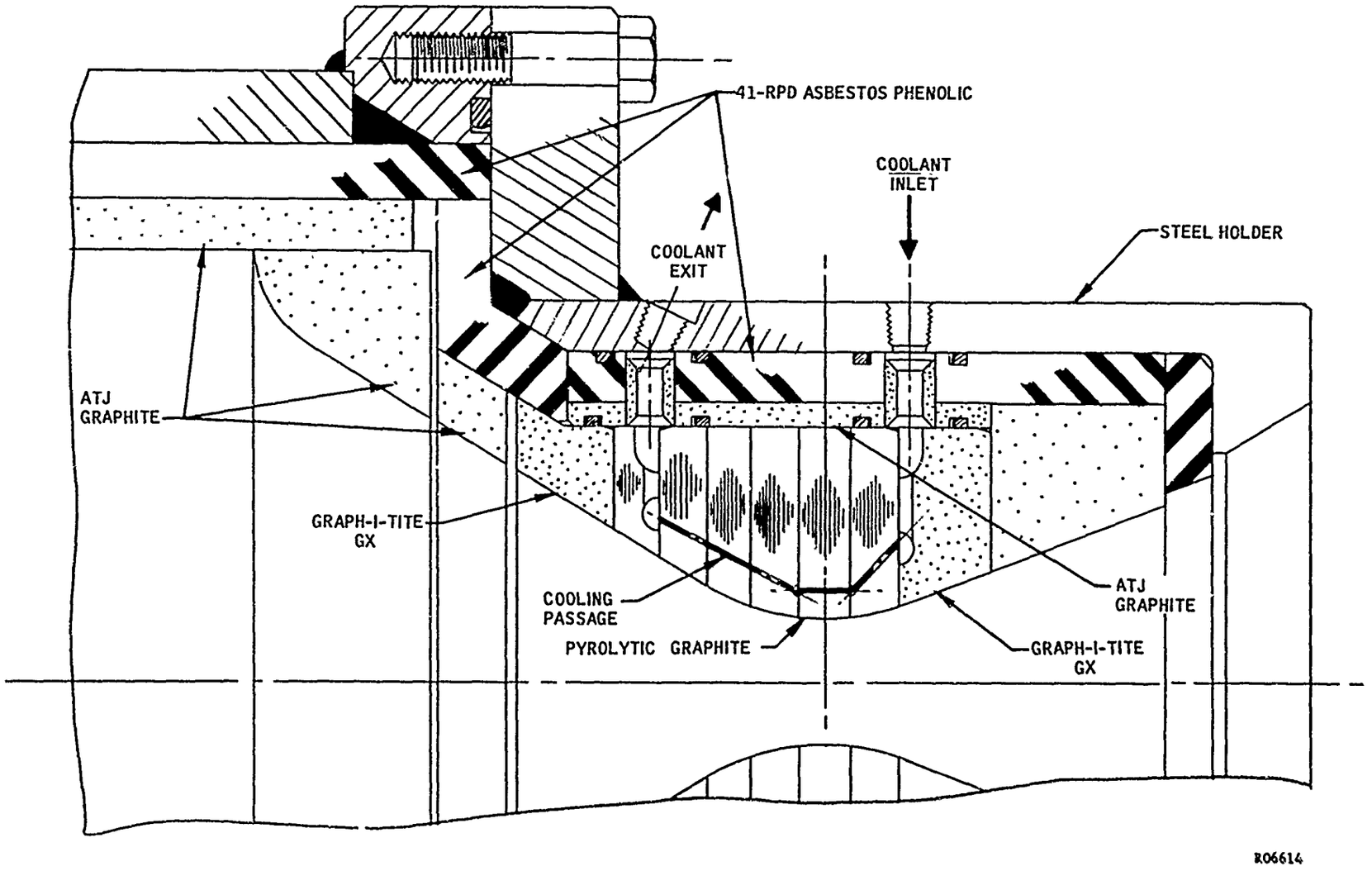

FIGURE 4-1. FIRST TEST NOZZLE

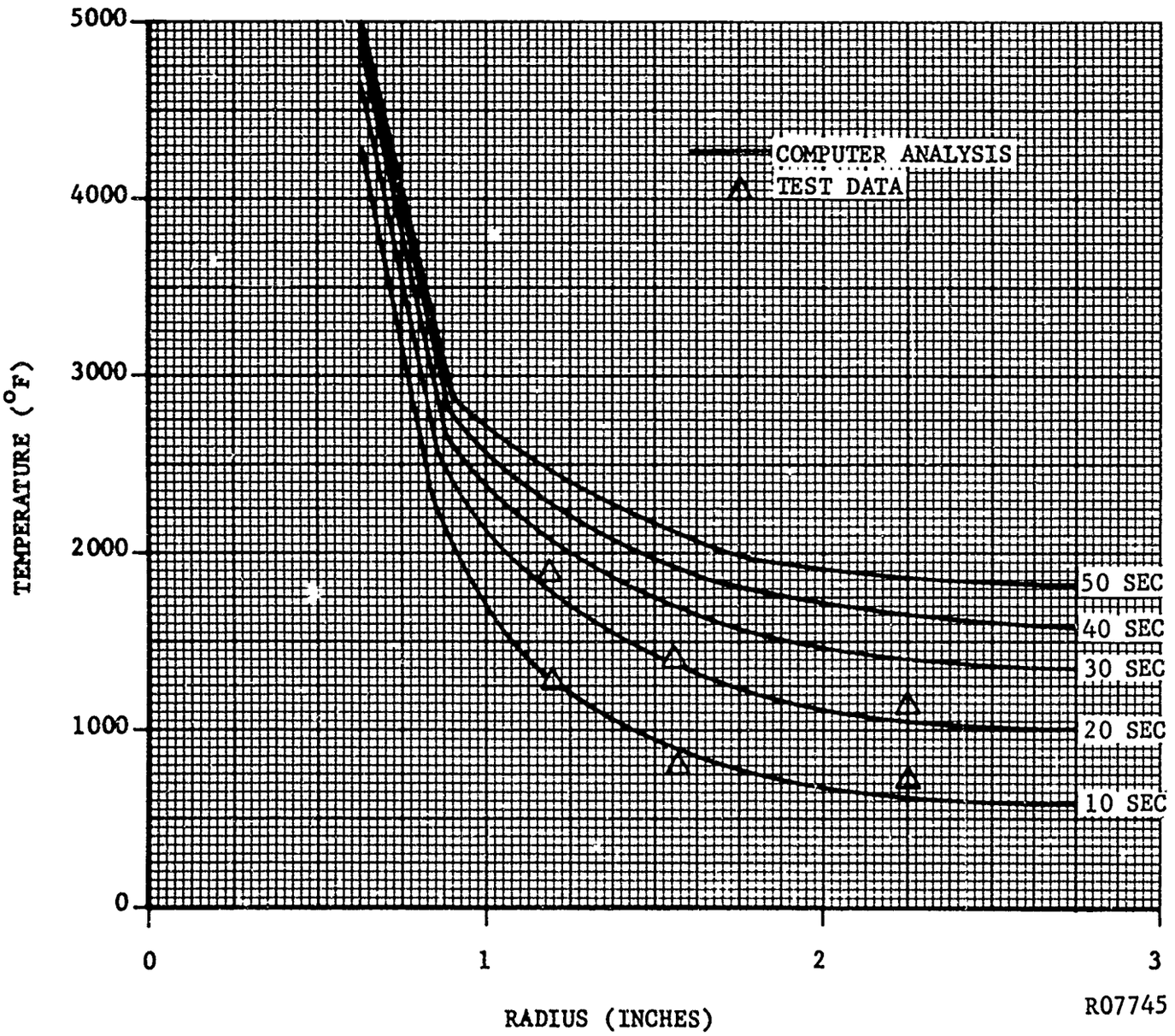

FIGURE 4-2. TEMPERATURE DISTRIBUTION FOR SUB-SCALE NOZZLE TEST NO. 1 IN THE THROAT WASHER

TABLE 4.1

FILM-PROTECTED, CONVECTION-COOLED SUBSCALE NOZZLE

TEST CONDITIONS

Test Number	1		2		3		4	
	Desired	Actual	Desired	Actual	Desired	Actual	Desired	Actual
Flow Rate, $-O_2$ (lbs/sec)	2.16	2.19	2.26	2.28	2.16	2.19	2.16	2.205
Flow Rate, $-N_2$ (lbs/sec)	0.81	0.80	0.825	0.829	0.81	0.81	0.81	0.80
Flow Rate, -Slurry (lbs/sec)	2.38	2.41	2.48	2.49	2.38	2.35	2.38	2.375
Flow Rate, -Total (lbs/sec)	5.35	5.40	5.565	5.599	5.35	5.35	5.35	5.380
Flow Rate, $-CH_4$ (lbs/sec)	0.0280	0.0283	0.0280	0.0280	0.0280	0.0265	0.0280	0.028
Chamber Pressure, P_c (psia)	700	715	700	695	700	703	700	686
Initial Throat Dia. (in.)	1.250	1.248	1.280	1.284	1.250	1.248	1.250	1.254
Duration of Run, t (sec)	50	21.5	50	50.6	50	51.4	50	37.8
Thrust, F (lbs)	1271		1361		1240		1269	
Characteristic Vel., C* (ft/sec)	5220		5180		5175		5067	
C* % Theoretical	98.1		97.3		97.3		95.2	

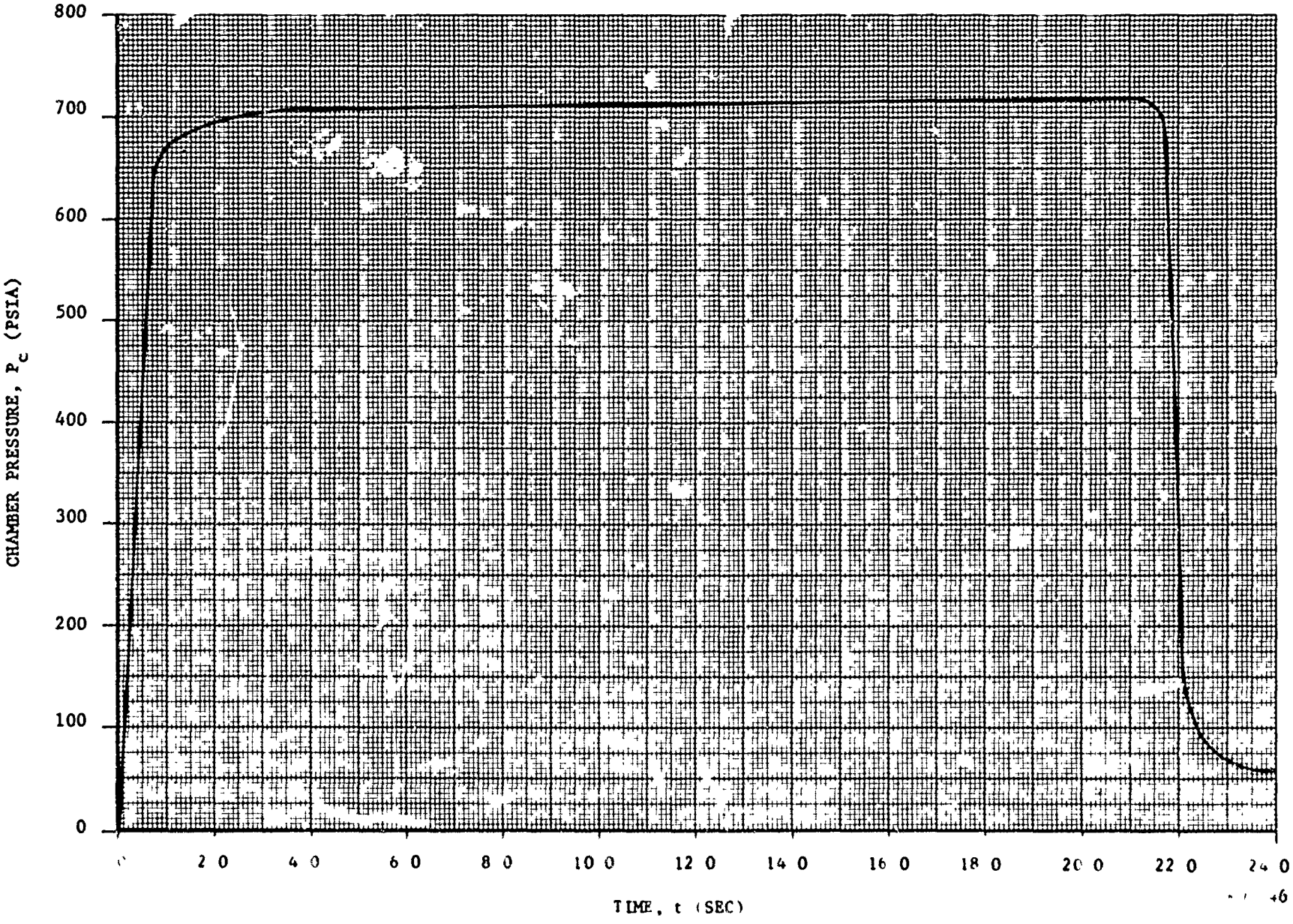
800
700
600
500
400
300
200
100
0
CHAMBER PRESSURE, P_c (PSIA)
2 0
4 0
6 0
8 0
10 0
12 0
14 0
16 0
18 0
20 0
22 0
24 0
TIME, t (SEC)

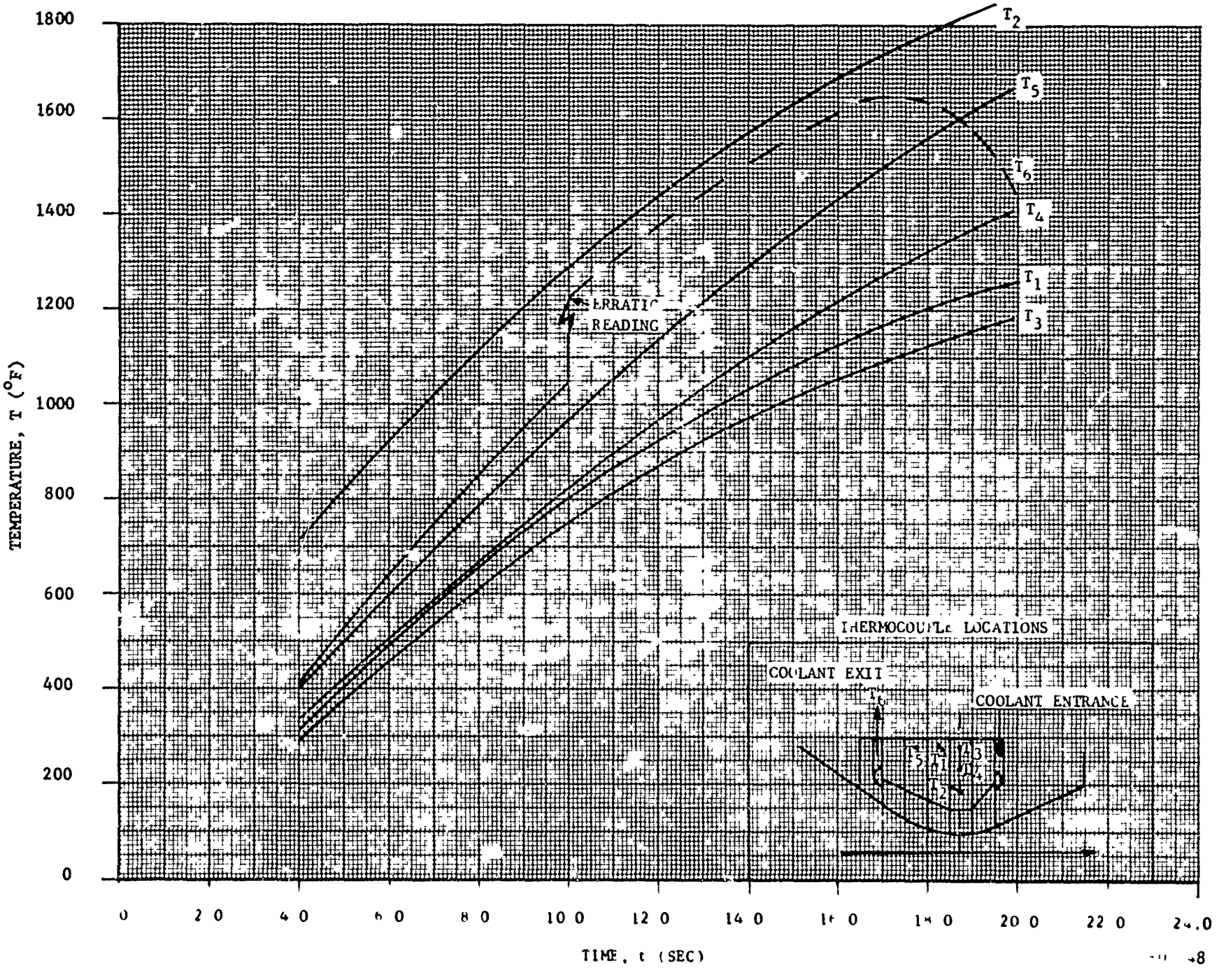

TEMPERATURE VERSUS TIME FOR S B-S ALLOY

TABLE 4.2

COMPARISON OF PREDICTED AND MEASURED TEMPERATURES IN ENTRANCE SECTION OF NOZZLE NO. 1

Temperature T_1 (r = 2.25 inches)

t (sec)	Computer Prediction (^oF)	Measured (^oF)
10	711	780
20	1182	1260

Temperature T_5 (r = 2.25 inches)

t (sec)	Computer Prediction (^oF)	Measured (^oF)
10	817	980
20	1334	1670

The test was terminated prematurely because of over pressure in the methane cooling manifold. This pressure was red-lined at 1000 psia because the primary function of its measurement was to indicate clogging of the cooling passages by the carbon particles formed from the dissociation of methane. Evaluation of the test data indicated that the methane overboard exhaust nozzle was too small. This nozzle was to have maintained the coolant pressure at 700 to 800 psia to duplicate the pressures to be obtained when injection would be involved. The nozzle was sized based on hand calculations of the characteristic velocity of a methane, carbon, and hydrogen mixture at the expected exhaust temperature. This obviously proved unsatisfactory. To resize the nozzle, a computer calculation was made to give the c* of the mixture as a function of temperature; the resultant curve is presented in Figure 4-5.

The pressure drop through the cooling passages was 35 psi at 8 seconds. No later measure was possible because the trace went off the chart due to the unexpectedly high pressure. As was predicted by laboratory tests (Reference 1), there was no carbon particle clogging. There was, however, some graphite deposition in the collection manifold at the coolant exit in the regions of low velocity. There was no evidence of clogging or flow restriction due to this deposition.

The average particle size of the carbon was 0.2 microns which is approximately the same as obtained in the laboratory tests.

(3) Discussion

Except for the methane exhaust nozzle sizing problem the test was completely successful for the short duration it was run. The measured temperatures were very close, in most cases, to predictions. There was no evidence of leakage of methane between washers to the surface even with the unusually high coolant pressure.

Because of the excellent appearance of the nozzle, it was decided to refire it. First, however, the nozzle was disassembled to replace O-rings which char badly during temperature soak back after termination. On dissassembly a radial crack was noted in the most upstream cooled washer which required replacing. The washer containing the collection manifold was replaced also so that the manifold could be reduced in size to possibly reduce graphite deposition by increasing the gas velocity.

No photographs were taken of the nozzle after testing since nothing of consequence could be shown.

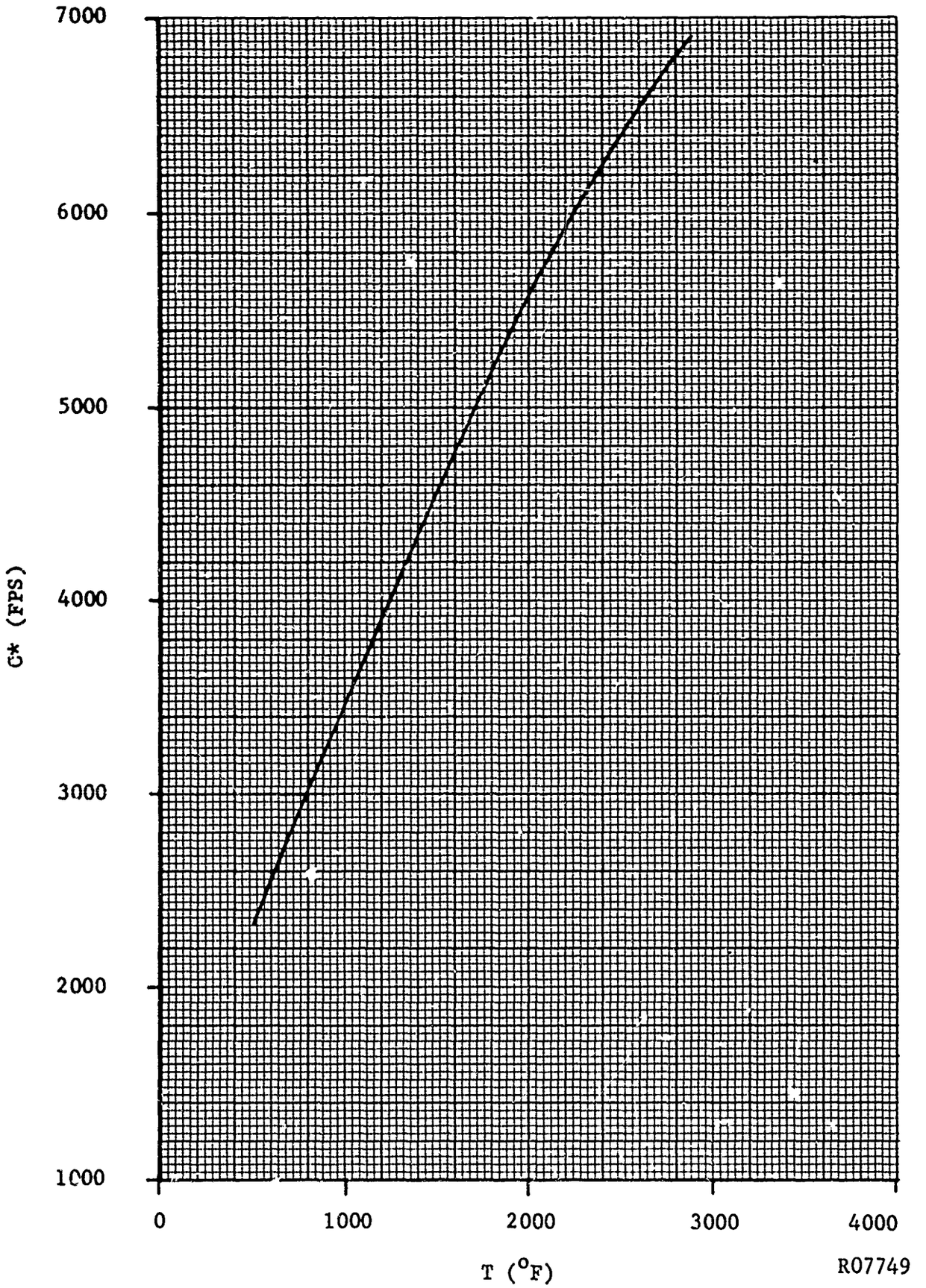

FIGURE 4-5. C* OF DISSOCIATED METHANE

b. Sub-Scale Nozzle Test No. 2

(1) Design Description

Since the nozzle from Test 1 was refurbished, the configuration is essentially identical to that shown in Figure 4-1. Because of the replacement of the two entrance section washers recontouring was required and approximately 0.015 inches of material was removed from the nozzle wall throughout.

A new methane exhaust nozzle was installed. Methane flow rate remained at 0.028 lb/sec.

(2) Test Results

The nozzle was run for a duration of 50.6 seconds at the conditions indicated in Table 4.1. The chamber pressure vs. time is shown in Figure 4-6 and the temperature histories are shown in Figure 4-7. The comparison of thermocouple data and predicted temperatures are shown in Figure 4-8 and in Table 4.3. Figure 4-9 shows the comparison between the heat actually absorbed by the methane and the calculated absorption based on computer results.

The chamber pressure decreased from 731 to 700 psia over the last 25 seconds which corresponds to a corrosion rate of 0.6 mil/sec for this period. Inspection of the nozzle after the test indicated severe localized corrosion over approximately a 90^{o} arc in the two washers immediately upstream of the throat. This corrosion had proceeded into the throat making it somewhat egg-shaped. This area of corrosion is shown in Figure 4-10 and, as can be seen, it went into the cooling passages which are approximately 0.25 inches from the wall. The methane manifold pressure indicated that the breakthrough probably occurred at 30 seconds which would require a corrosion rate of 8.3 mils/sec. Figure 4-11 shows the opposite side of the nozzle throat region which is relatively uncorroded. Because of the egg-shaped configuration accurate measurement of the less corroded areas were not possible however rough measurements indicated a 5 to 10 mil dimensional change.

Deposition of graphite again occurred in the manifolds at a rate of approximately 0.2 mils/sec but apparently caused no difficulty.

Prior to the apparent breakthrough into the cooling passage the coolant pressure drop through the passage had stabilized at approximately 75 psid.

(3) Discussion

As is noted in Figure 4-6, chamber pressure varied from 695 psia up to 731 psia at 25 seconds then down 700 psia at the termination of the test at 50 seconds. Flow rates of propellants were constant throughout the test.

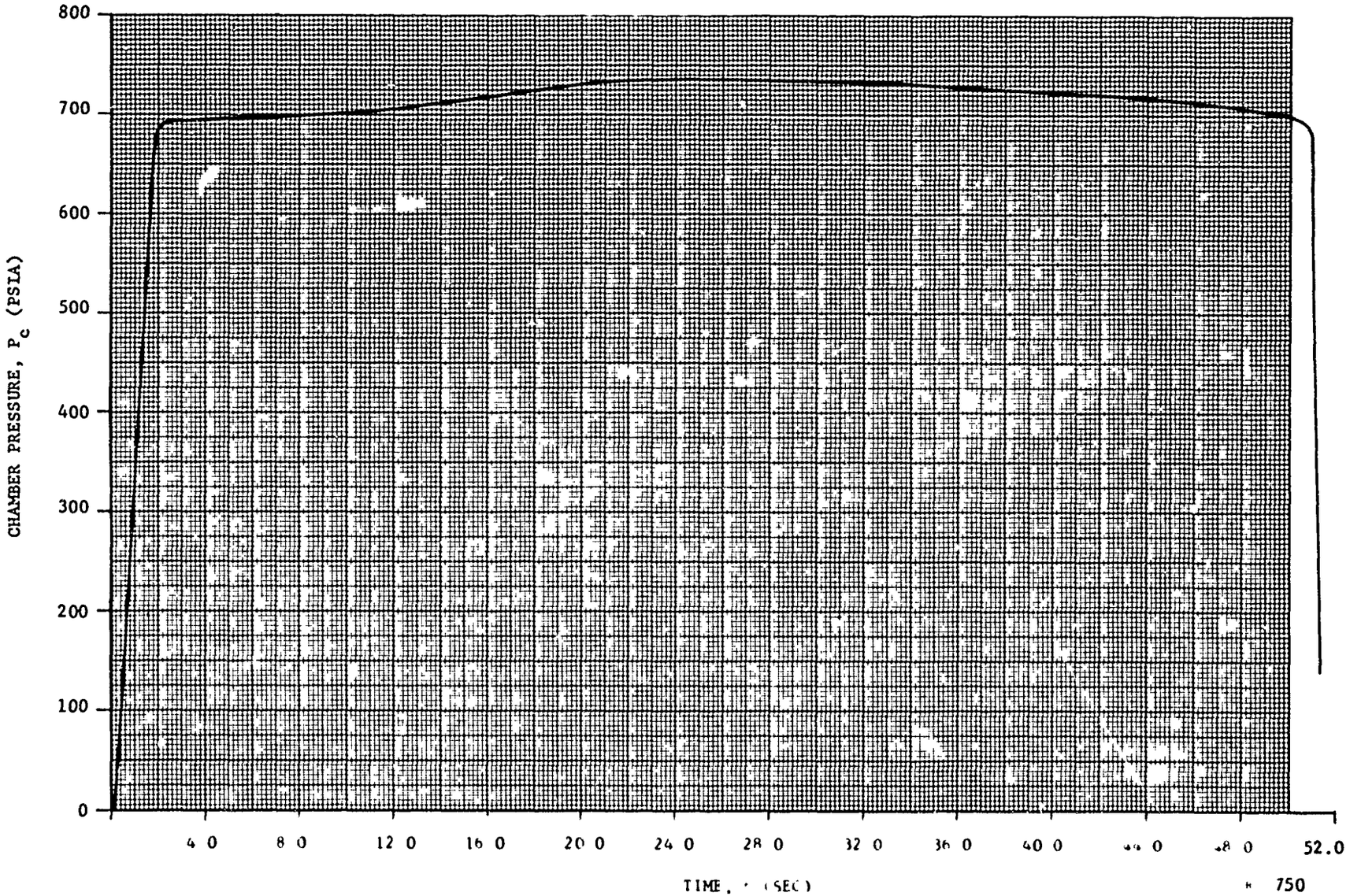

FIGURE 4-6. CHAMBER PRESSURE VERSUS TIME FOR SUB-SCALE NOZZLE TEST 2

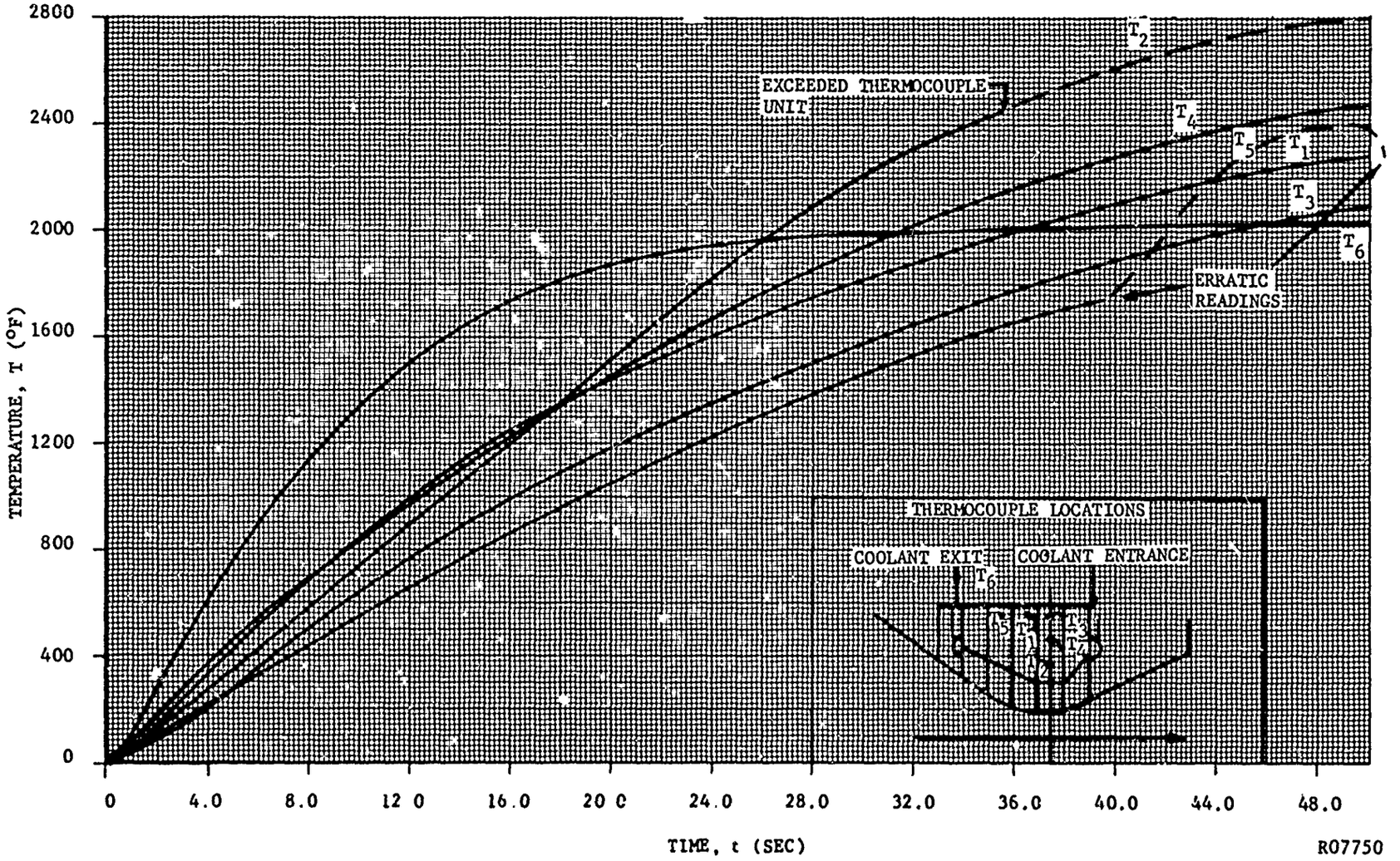

FIGURE 4-7. TEMPERATURE VERSUS TIME FOR SUB-SCALE NOZZLE TEST 2

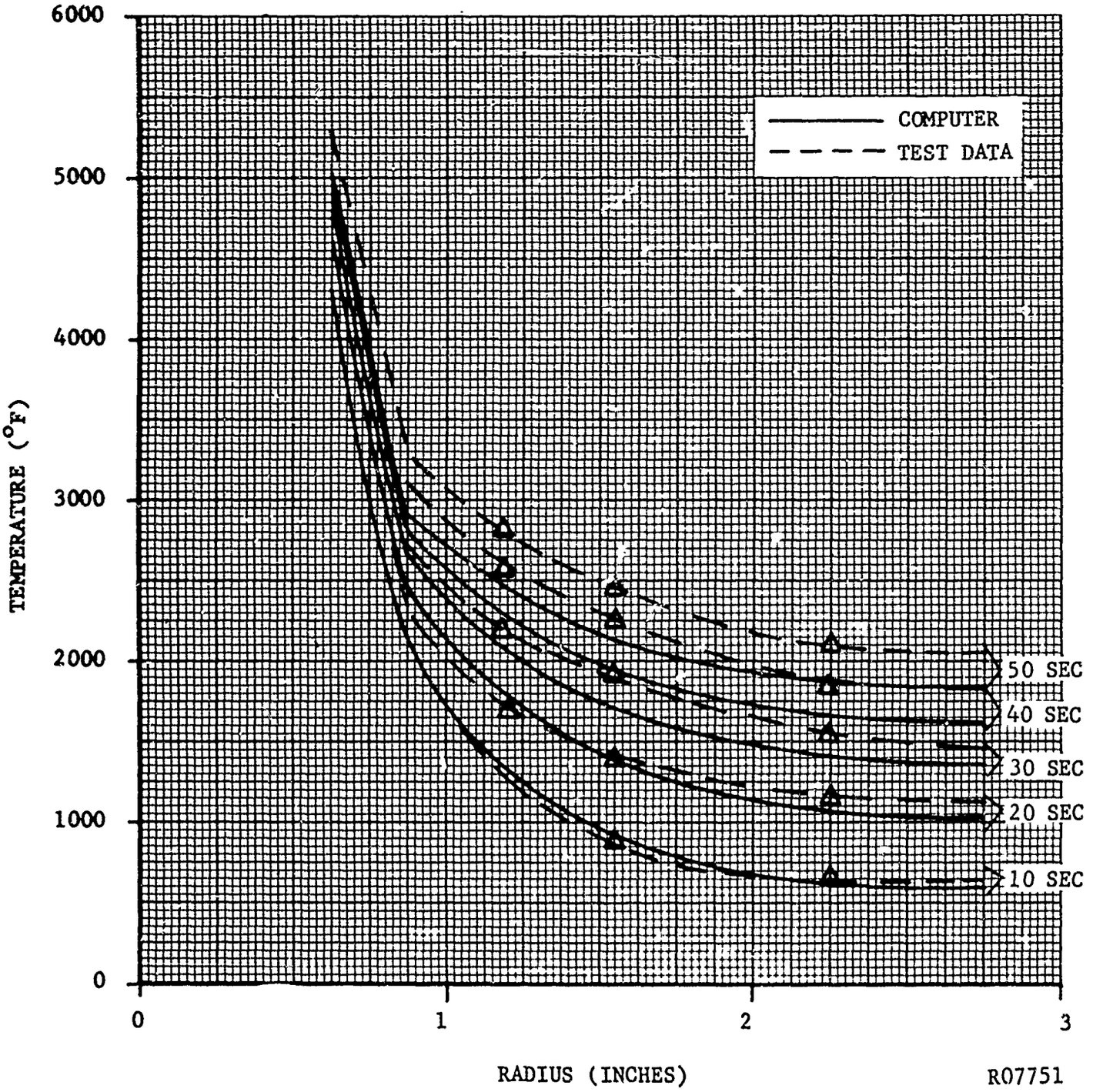

FIGURE 4-8. TEMPERATURE DISTRIBUTION FOR SUBSCALE NOZZLE TEST NO. 2 IN THE THROAT WASHER

TABLE 4.3

COMPARISON OF PREDICTED AND MEASURED TEMPERATURES IN ENTRANCE SECTION OF NOZZLE NO. 2

Temperature T_1 (r = 2.25 inches)

t (sec)	Computer Prediction (^oF)	Measured (^oF)
10	711	840
20	1182	1440
30	1534	1820
40	1820	2100
50	2059	2300

Temperature T_5 (r = 2.25)

t (sec)	Computer Prediction (^oF)	Measured (^oF)
10	817	540
20	1334	1060
30	1719	1470
40	2025	1760
50	2280	--

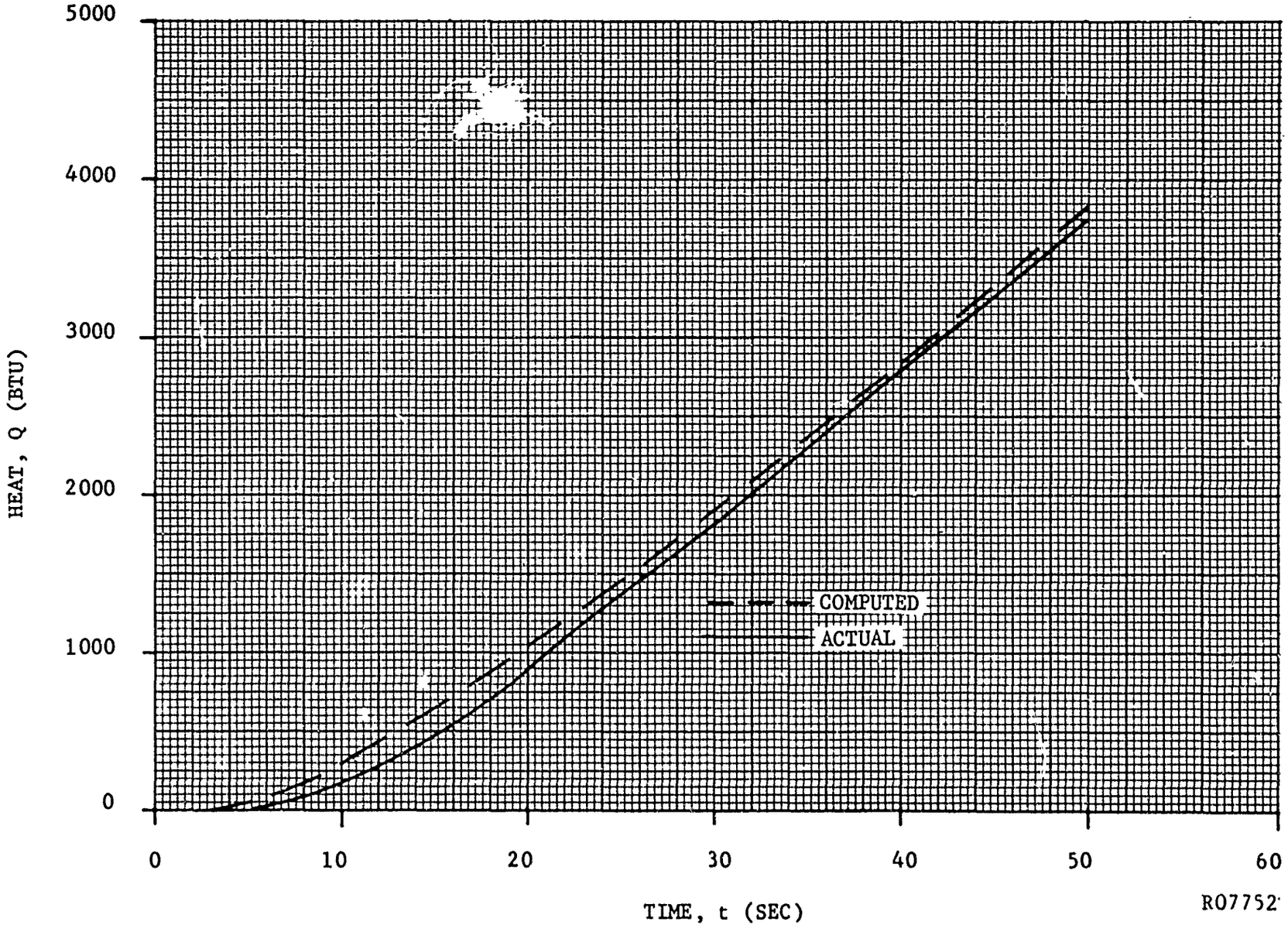

FIGURE 4-9. HEAT ABSORBED BY COOLANT VERSUS TIME IN TEST NO. 2

FIGURE 4-10. ENTRANCE AND THROAT SECTION SHOWING LOCALIZED CORROSION UP STREAM OF THROAT AFTER TEST 2.

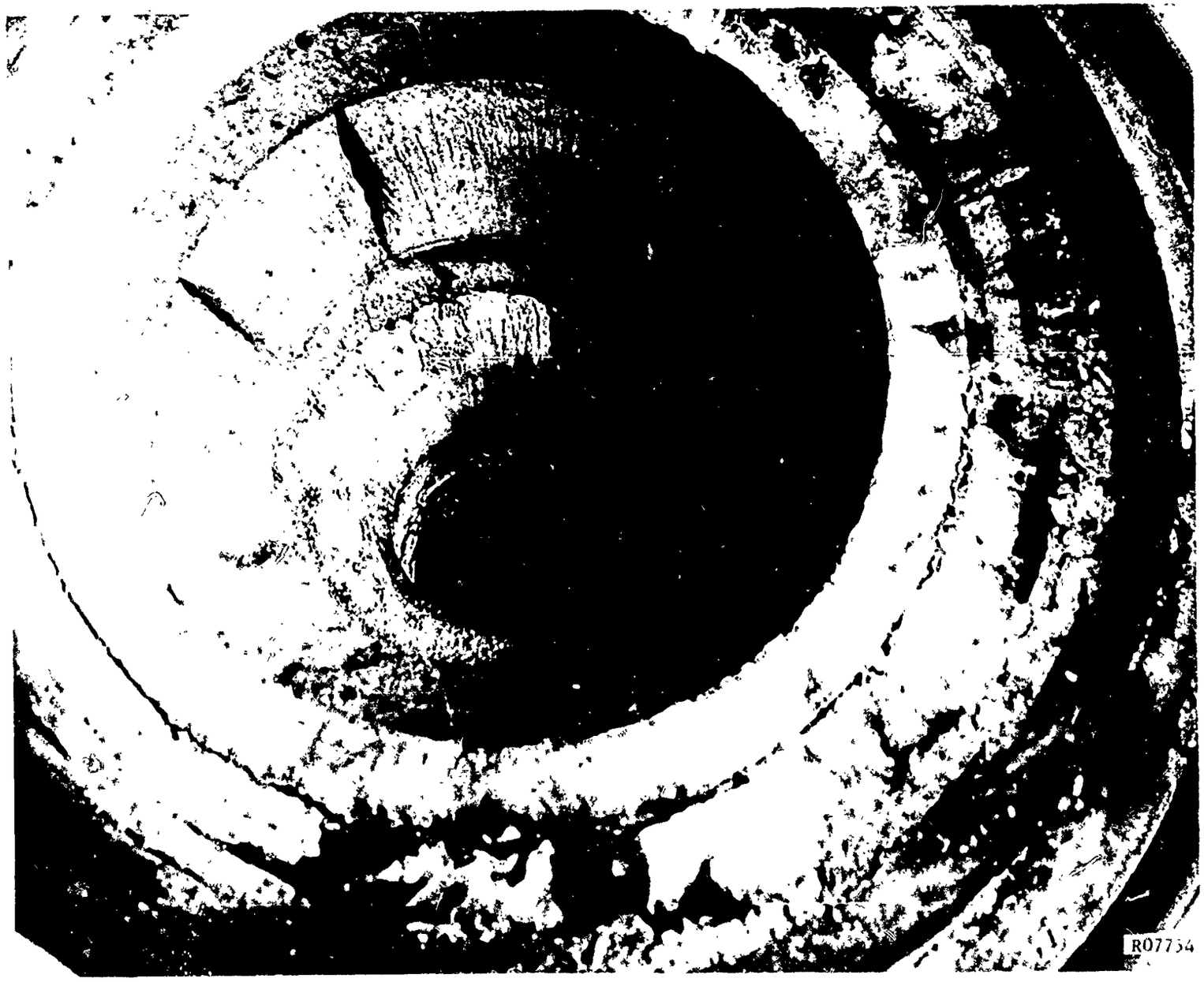

FIGURE 4-11. ENTRANCE AND THROAT REGION AFTER TEST NO. 2
SHOWING SIDE OPPOSITE LOCAL CORROSION

This hump has been noted previously in tests involving pyrolytic graphite washer-type heat sinks. It appears to be caused by plastic deformation resulting from thermal expansion which causes a decrease in throat diameter. Since there is a steep temperature gradient in the material, higher thermal expansion at the wall will obviously create higher stresses and, at the high temperatures present, dimensional change would tend to take place in the unrestrained direction which is inward. Another mechanism which would have the same effect is permanent "c" direction contraction and "a" direction expansion which occurs when pyrolytic graphite is heated above its deposition temperature of around 3800°F. This effect is time dependent and significant change does not occur below 5000°F. Since the nozzle wall temperature was designed to operate at a maximum of 5100°F to 5200°F it is doubtful if the effect would be significant in a 50 second test. Also no "c" direction contraction was observed after disassembly of the nozzle. Alumina deposition can be discounted since the wall temperature was too high.

The entrance section surface regression was originally thought to result from a pyrolytic graphite structural failure since it was localized and could not have been caused by corrosion by the propellant gases. It is now believed (after seeing the results of Tests 3 and 4) that the regression was caused by hydrogen corrosion. Re-examination of the nozzle indicated a strong possibility of a leak from the collection manifold upstream of the attacked area. At the manifold the methane is mainly dissociated to carbon and hydrogen. Leakage through a small passage would probably result largely in hydrogen with the carbon filtered out.

The thermocouples in the entrance section were located in the region of the corroded area hence their measurements are questionable. The effect on the measurements in the throat region is not known. The coolant heat absorption comparison is also of no consequence since leakage into the main stream would invalidate the calculations.

c. Nozzle Test No. 3

(1) Design Description

The configuration of the nozzle for the third test is shown in Figure 4-12. The concept for this nozzle was to convectively cool with methane then inject through 28 discrete holes in the entrance section of the nozzle at an area ratio of 3.0. It was the purpose of the test to determine the increase in effectiveness of film injection over that of temperature control on corrosion reduction.

The throat section washers for this test had an outside diameter of 3.00 inches and were backed by ATJ graphite. Convection passage geometry was

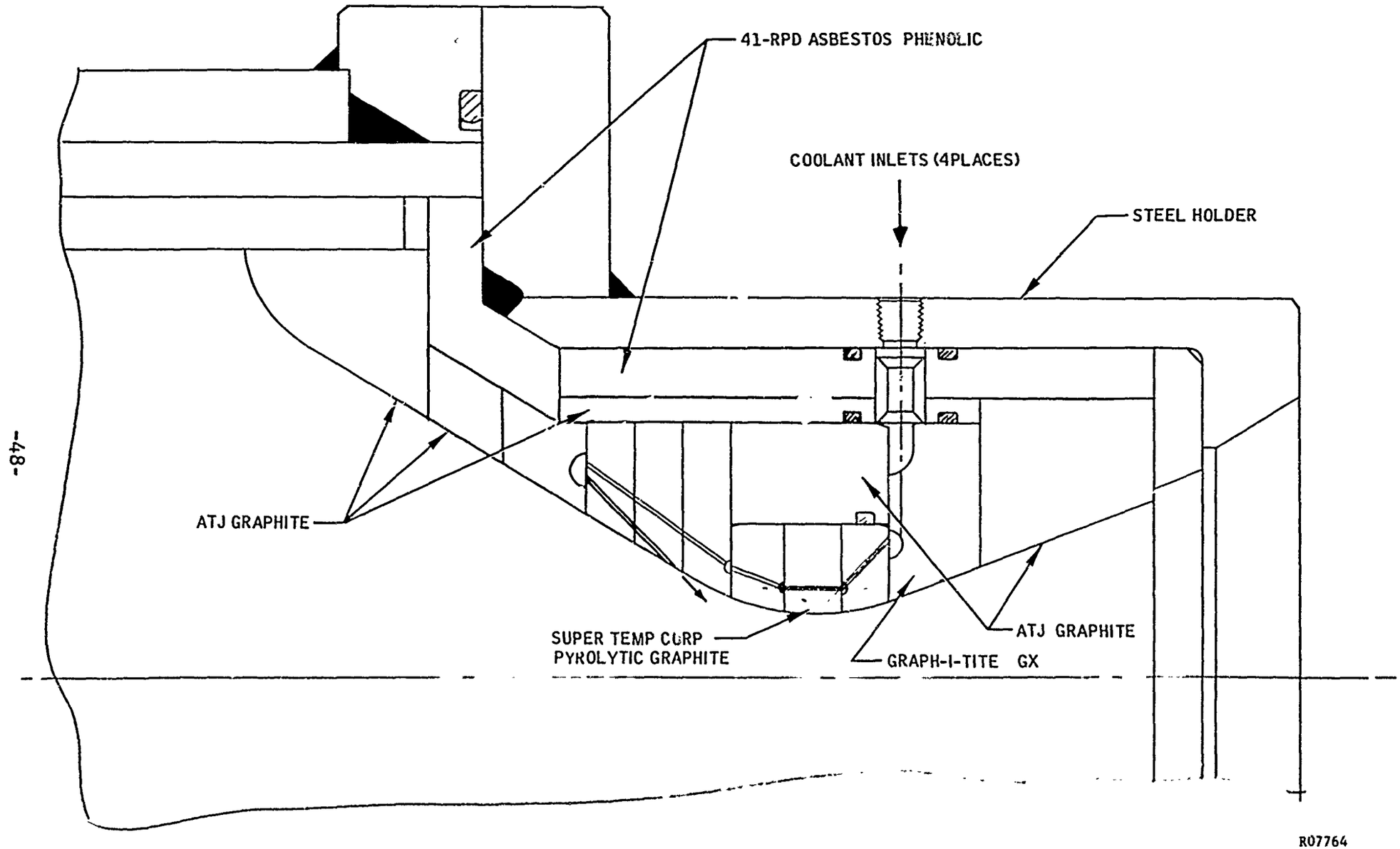

FIGURE 4-12. NOZZLE DESIGN FOR TEST 3

similar to that in the first two tests. The coolant flow rate was the same as in the previous tests.

(2) Test Results

The nozzle was run for 51.4 seconds at the conditions shown in Table 4.1. The chamber pressure vs. time is shown in Figure 4-13 and the temperature histories are shown in Figure 4-14. Only one thermocouple measurement was successfully obtained in the throat washer. A spring loaded platinum-platinum, rhodium thermocouple blew out on ignition, however it did not cause the test to be aborted.

As can be seen in Figure 4-13, the chamber pressure started falling very rapidly at 28 seconds. A very severe regression rate occurred as is indicated in Figure 4-15. The regression rate was calculated from the rate of change of chamber pressure assuming a constant c*. The final throat diameter arrived at by this procedure compared very closely with the measured diameter after the test. Entrance section regression immediately upstream of the throat was more severe than the throat (see Figure 4-16).

The methane coolant pressure was very erratic with apparent loss of injection at 36 seconds.

Comparison of measured temperatures with values predicted by computer calculations are given in Figure 4-17 and Table 4.4.

(3) Discussion

As can be seen in Figure 4-15 the regression rate of the pyrolytic graphite experienced was considerably greater than that generally experienced with an uncooled nozzle (Reference 7). It was first thought that the erratic coolant system operation and high regression rate was the result of a gross mechanical failure of the nozzle. However, inspection of p.g. washers failed to turn up any supporting evidence. There were only very minor delamination and no radial cracking. This latter observation alone indicates that the regression was not due to extremely high wall temperatures (6000°F and greater) which would result from an uncooled condition. In the past, uncooled heat sinks run for 50 seconds with theoretical wall temperatures of 5800°F have been grossly delaminated and has given evidence of local annealing at the surface (i.e. "c" direction shrinkage). These observations led to the conclusion that the injected dissociated methane corroded the p.g. at relatively low temperature.

The theory that the corrosion occurs at temperatures down toward 3000°F to 3500°F is supported by the fact that regression occurred all the way to the convection cooling passages. This, however, brings up an interesting

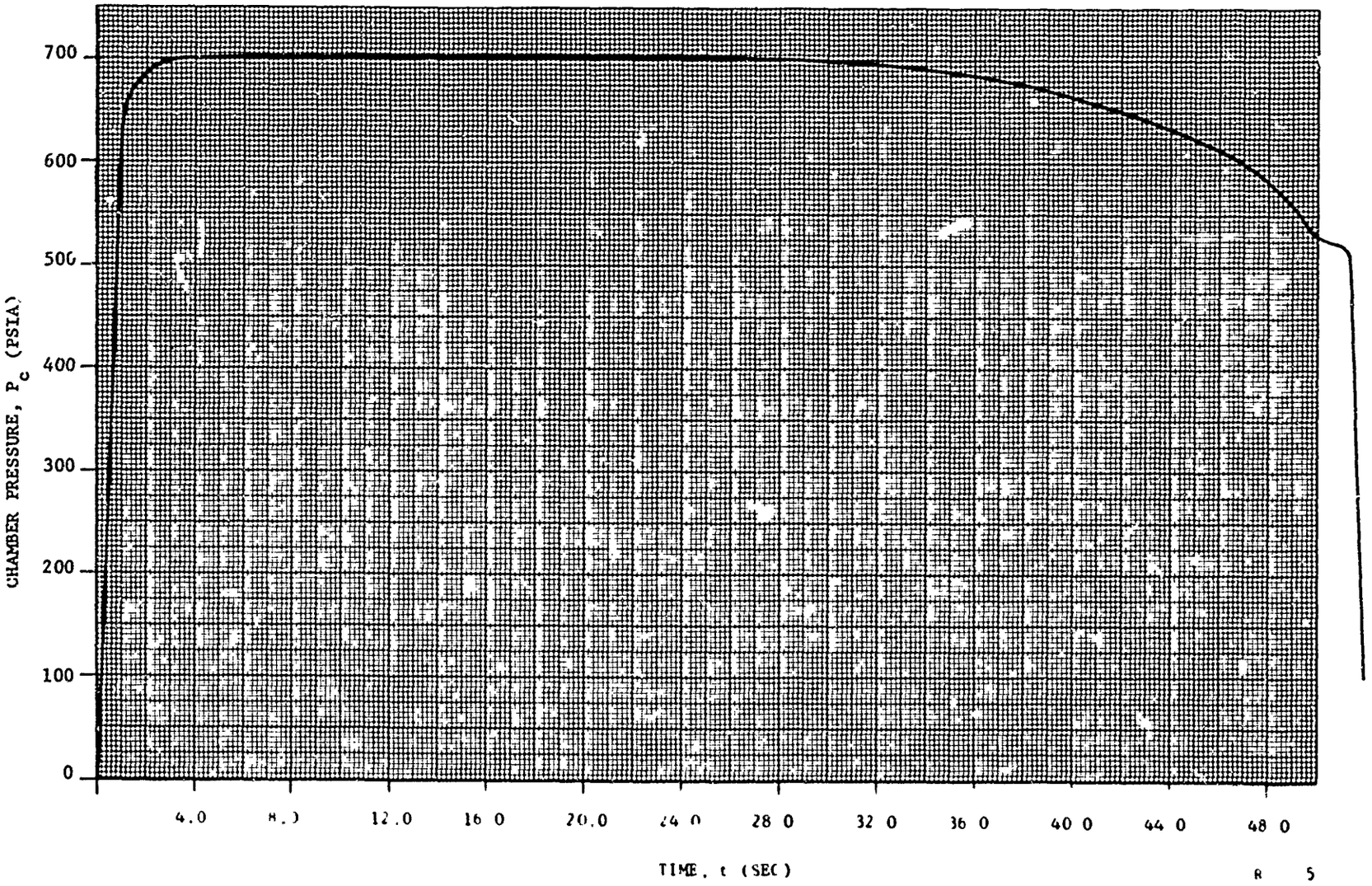

FIGURE 4-13. CHAMBER PRESSURE VERSUS TIME FOR NOZZLE TEST NO. 3

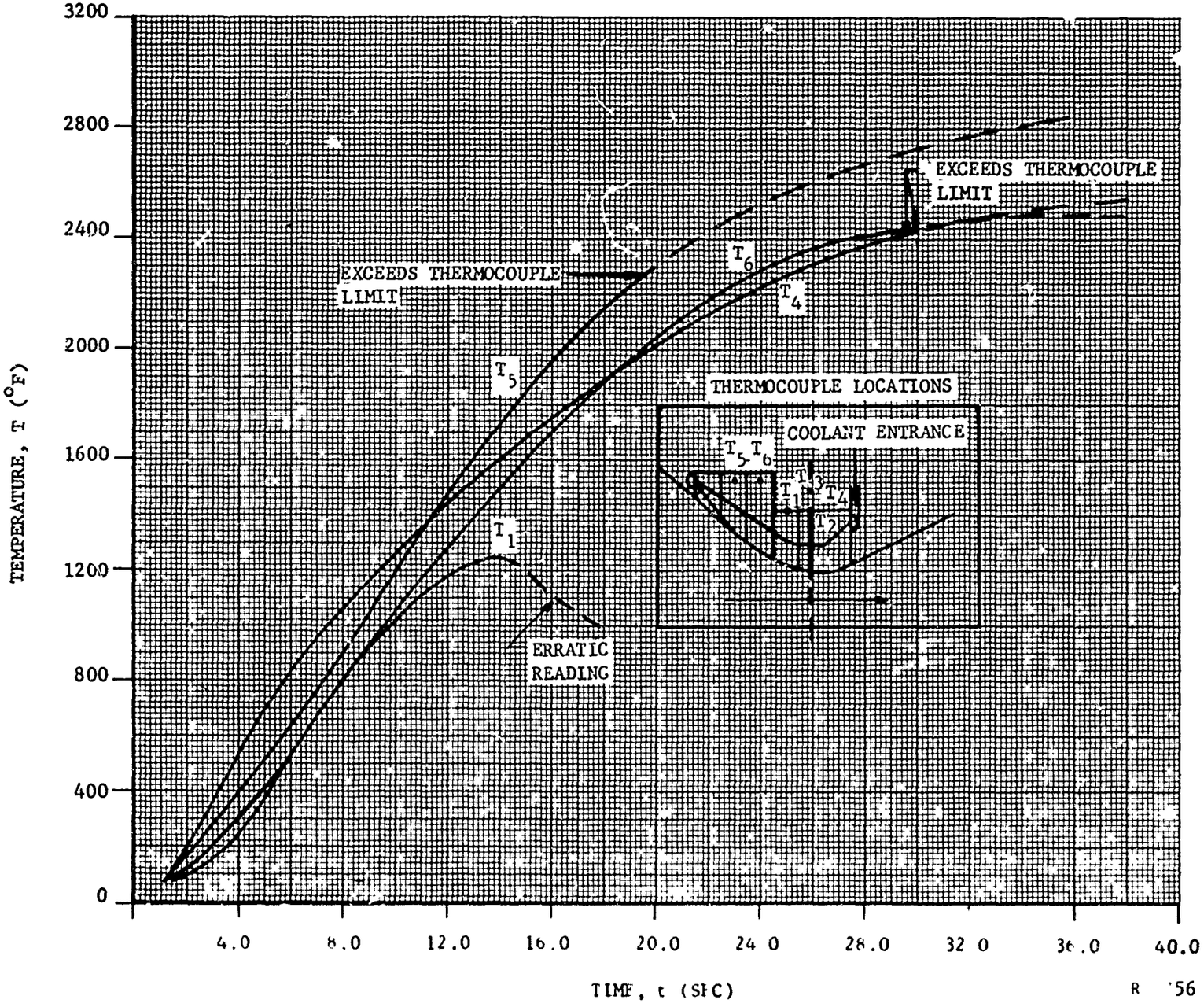

R '56

FIGURE 4 - TEMPERATURE VERSUS TIME FOR NOZZLE TEST NO. 1

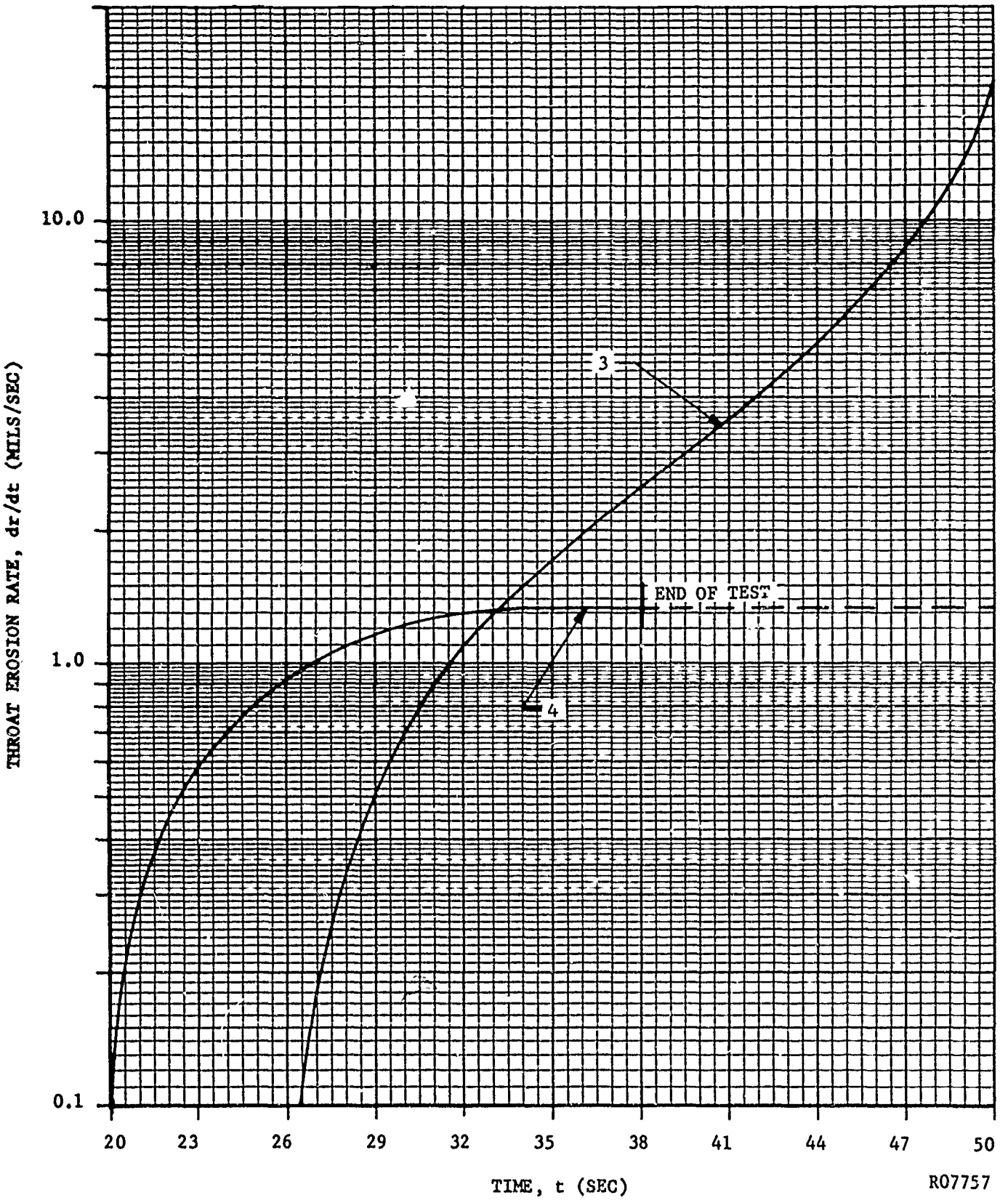

FIGURE 4-15. NOZZLE THROAT EROSION RATE FOR TEST 3 and TEST 4

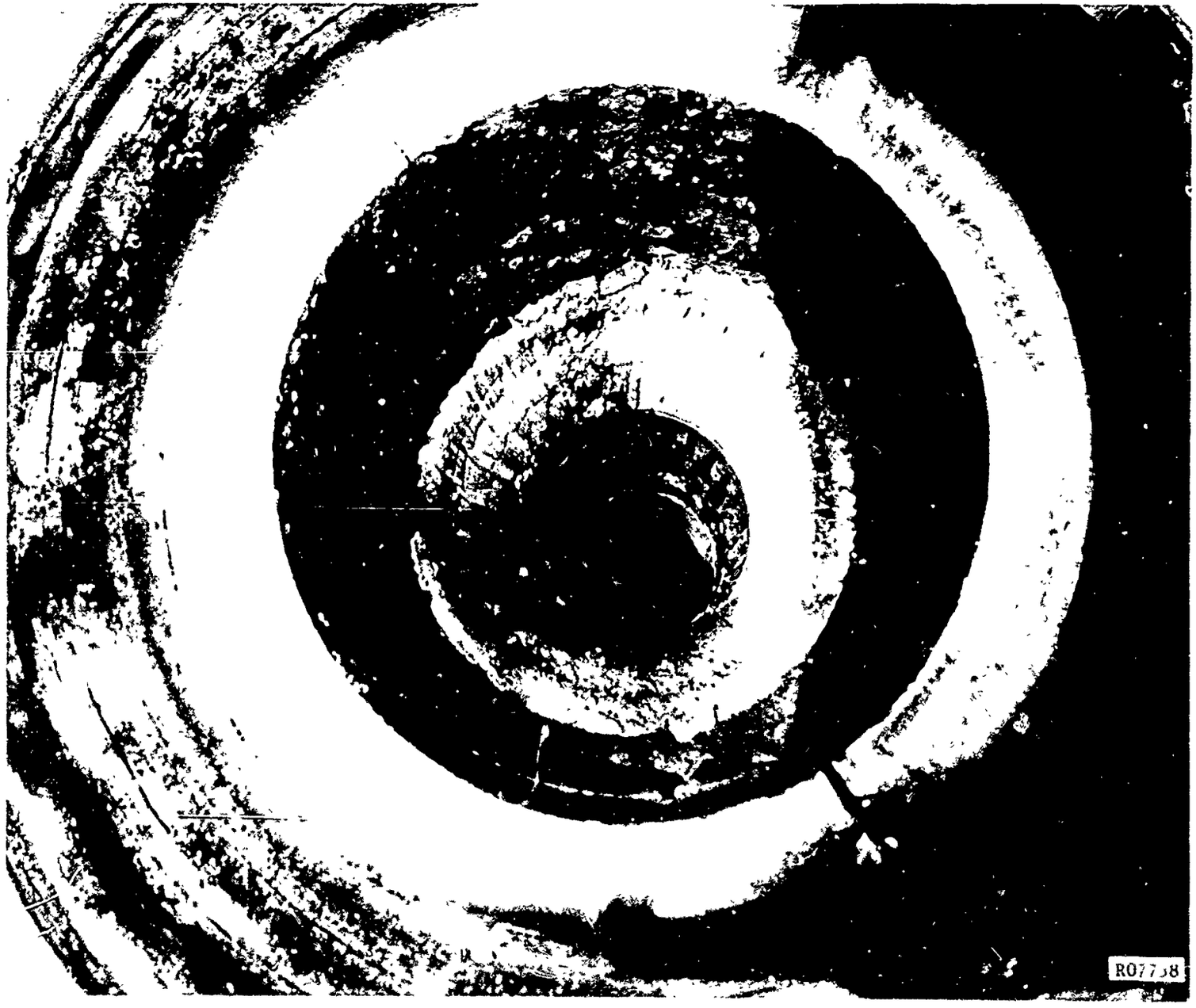

FIGURE 4-16. VIEW OF ENTRANCE AND THROAT SECTION OF NOZZLE AFTER TEST 3

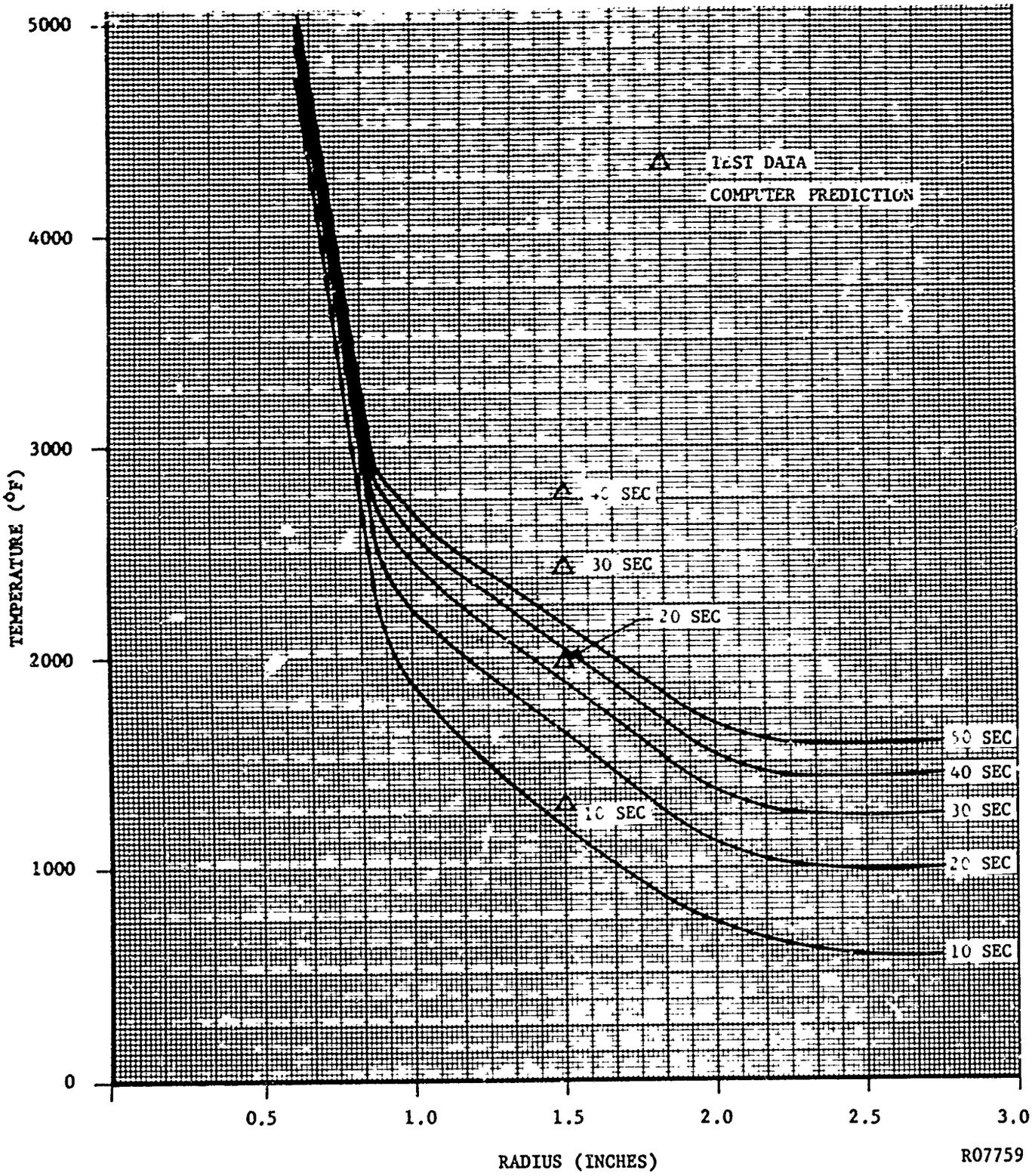

FIGURE 4-17. TEMPERATURE VERSUS RADIUS AT VARIOUS RUN TIMES FOR NOZZLE TEST NO. 3

TABLE 4.4

COMPARISON OF PREDICTED AND MEASURED TEMPERATURES IN ENTRANCE SECTION OF NOZZLE NO. 3

Temperature T_5 (r = 2.25 inches)

t (sec)	Computer Prediction (^oF)	Measured (^oF)
10	922	1200
20	1468	2300
30	1860	--
40	2160	--
50	2398	--

Temperature T_6 (r = 2.25 inches)

t (sec)	Computer Prediction (°F)	Measured (°F)
10	814	1280
20	1328	2050
30	1699	2440
40	1987	--
50	2217	--

question: why does the injected methane attack the p.g. on the hot gas side, whereas there is no evidence of enlargement of the convection holes. One explanation is that in the passages the hydrogen and carbon dissociation products of methane are, in fact, in equilibrium, whereas upon injection the carbon remains in a center core while the hydrogen diffuses radially giving a hydrogen rich annulus around the injection stream. There are possibly other fluid dynamic effects which could also give similar results.

As is noted when Table 4.4 is compared to Table 4.3, the injection of methane caused a significant increase in the temperature measurements. It is believed that this increase results from either surface regression which reduces the thickness of material between the thermocouple and the surface or a large increase in convection heat transfer coefficient due to injection of a good heat transfer medium.

d. Nozzle Test No. 4

(1) Design Description

The configuration of the fourth nozzle tested, as shown in Figure 4-18, was quite similar to the nozzle for Test 3. Since at the time it was not realized that methane corrosion was probably the cause of the failure of Test 3, the coolant conditions of the test were repeated in Test 4. Also it was felt that a test terminated at first indication of throat area change would aid greatly in the determination of the failure mode if it were other than a coolant system failure.

(2) Test Results

The nozzle was run for 37.8 seconds at the conditions shown in Table 4.1. The chamber pressure vs. time is shown in Figure 4-19 and the temperature histories are shown in Figure 4-20.

The throat corrosion was not as severe in this test as in the previous (see Figure 4-15) however the entrance section corrosion was again quite severe, as can be seen in Figure 4-21.

Entrance section temperature comparison cannot be made for this test with any degree of reliability because a computer run of this configuration has not been made. However the throat section temperatures should be consistent with previous calculations. This comparison is shown in Figure 4-22.

(3) Discussion

The results of this test fairly well substantiated the problem of increased corrosion due to methane injection. Again temperature measurement

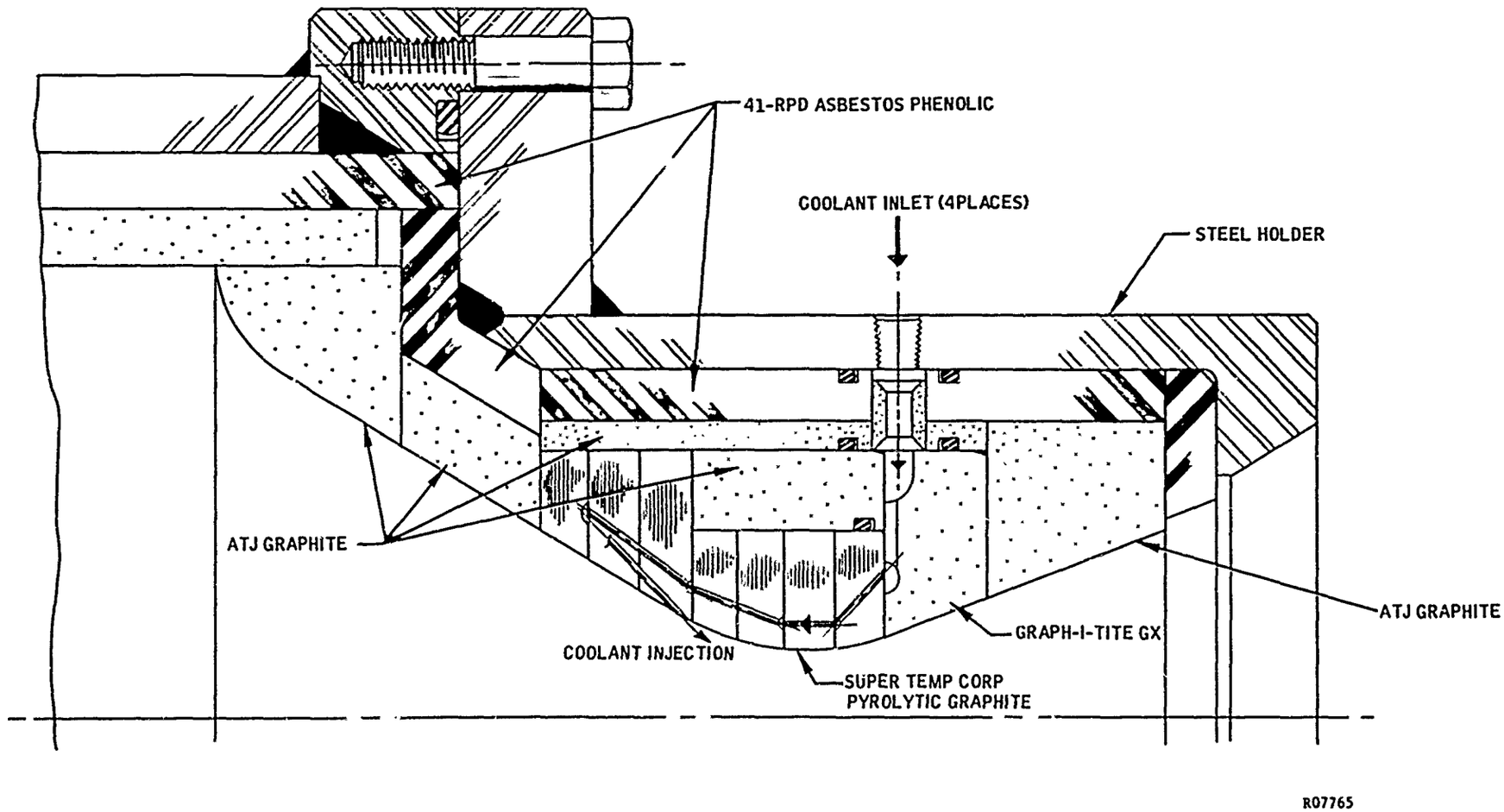

FIGURE 4-18. NOZZLE DESIGN FOR TEST 4

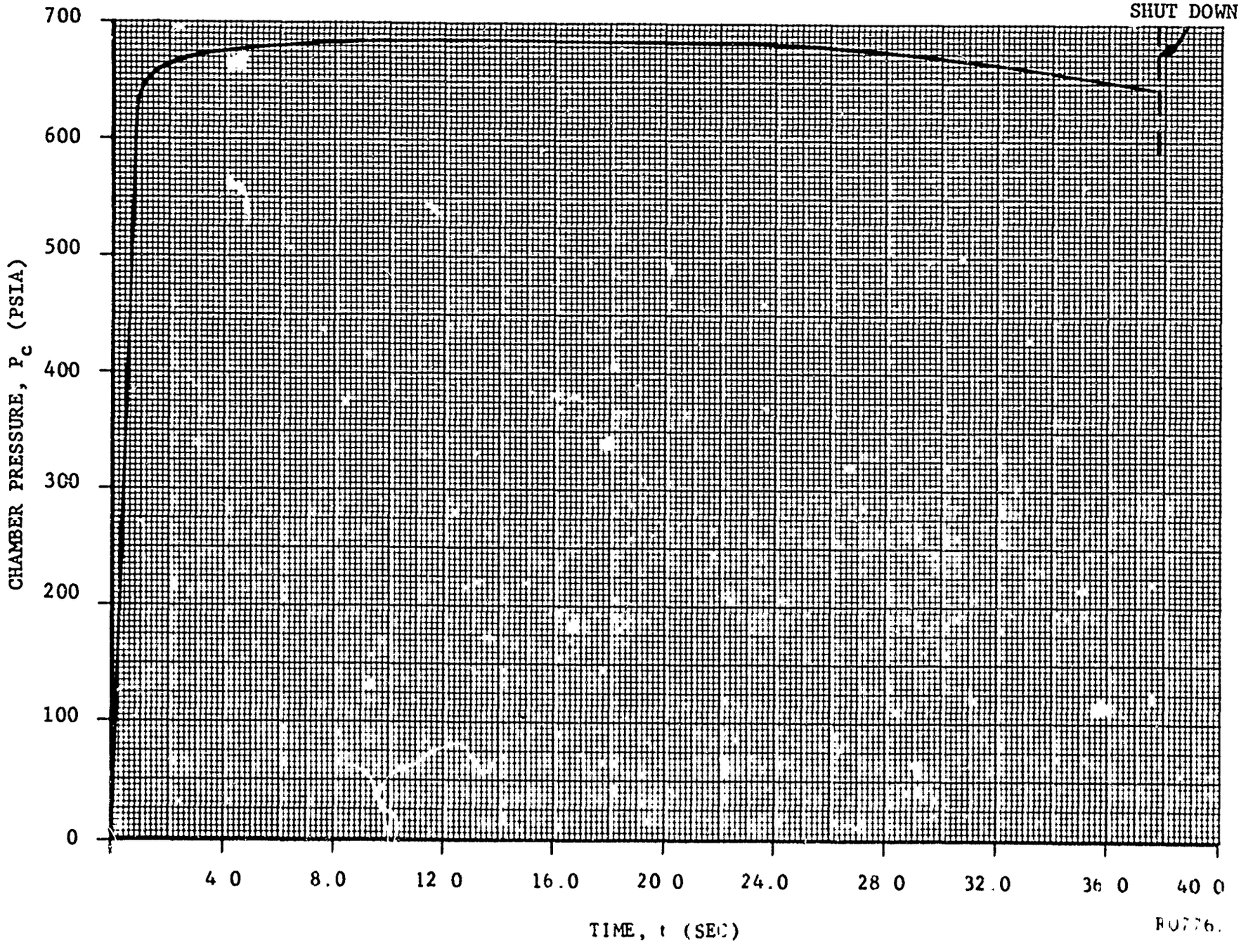

FIGURE 4-19 CHAMBER PRESSURE VERSUS TIME FOR NOZZLE TEST NO. 4

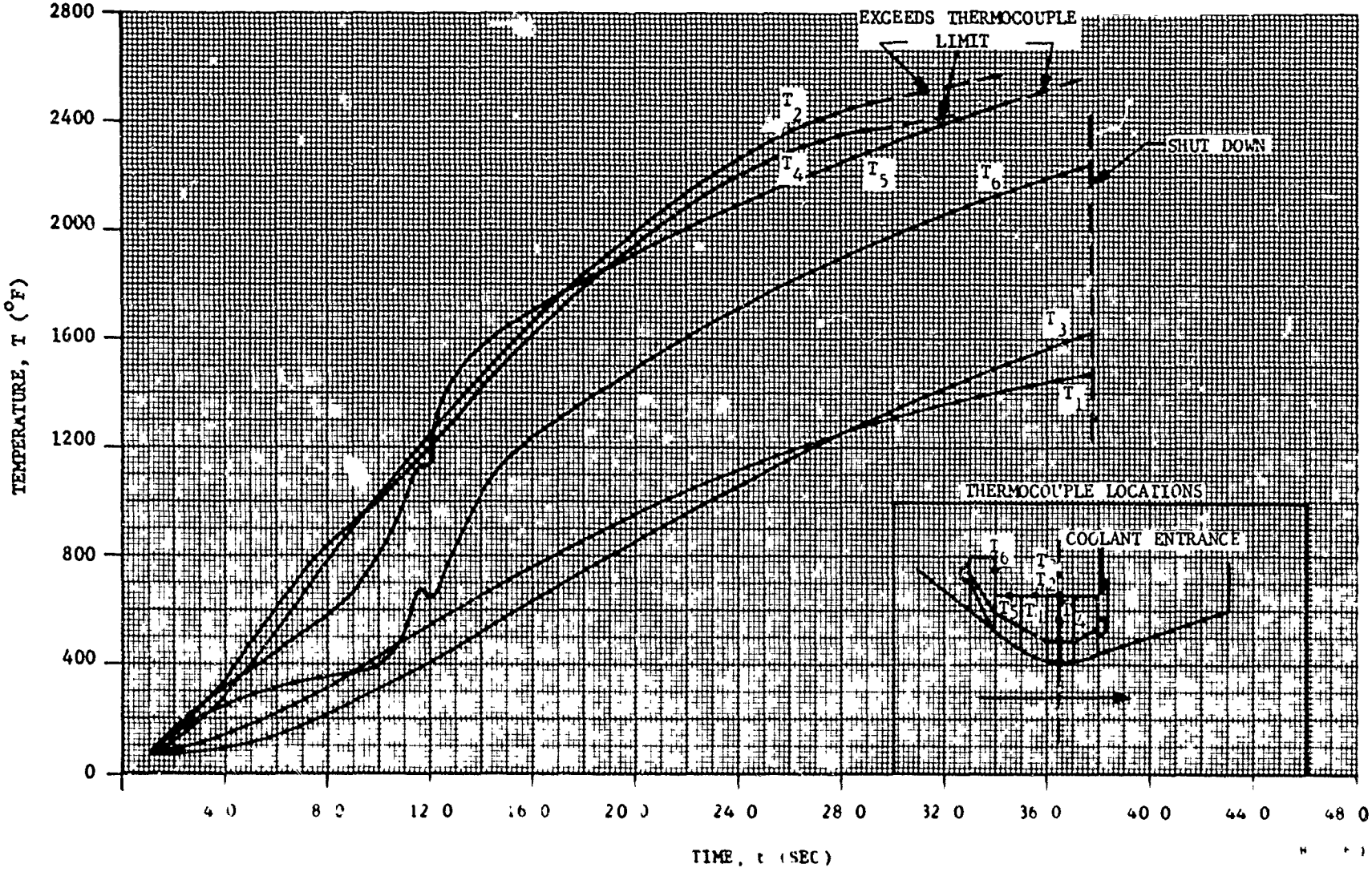
EXCEEDS THERMOCOUPLE LIMIT
SHUT DOWN
T_2
T_4
T_5
T_6
T_3
T_1
THERMOCOUPLE LOCATIONS
COOLANT ENTRANCE
TEMPERATURE, T (°F)
TIME, t (SEC)
2800
2400
2000
1600
1200
800
400
0
4 0
8 0
12 0
16 0
20 0
24 0
28 0
32 0
36 0
40 0
44 0
48 0

R07762

FIGURE 4-21. ENTRANCE AND THROAT SECTION OF NOZZLE AFTER TEST NO. 4

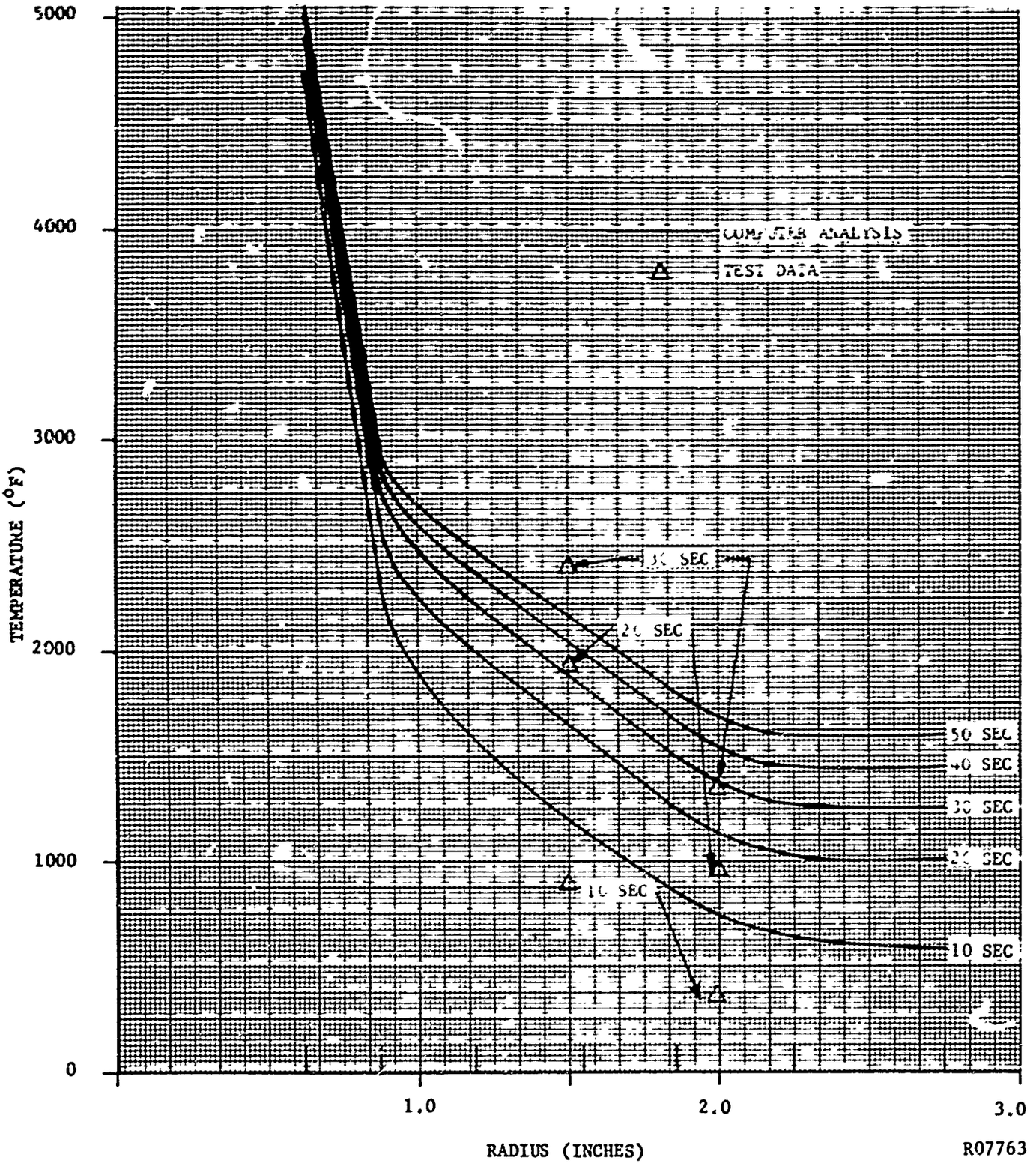

FIGURE 4-22. TEMPERATURE VERSUS RADIUS AT VARIOUS RUN TIMES FOR THROAT SECTION FOR TEST NO. 4

throughout the nozzle were higher than computer analyses have predicted. Corrosion rates were again quite high, however as noted in Figure 4-15, the throat regression rate was lower at test termination than in the previous test at the same time. In fact, the rate appeared to level out at 1.3 mils/sec. At present no good reason can be given for this occurrence.

Another unexplained phenomenon is the sudden jump in the two entrance section temperatures (see Figure 4-20) at approximately 10 seconds.

The appearance of the pyrolytic graphite in this test, as in the previous one, did not indicate excessive temperatures. There was very minor delamination and no radial cracking.

The washer immediately downstream of the throat had little or no surface regression and, in fact, had about a 10 mil coating of alumina over some of its surface.

As a result of Tests 3 and 4, it has been decided that the fifth test will utilize helium as a coolant/injectant with the same nozzle geometry as in Test 4. This will show conclusively if the methane is chemically attacking the p.g. as is indicated from the test results to date. Helium was selected since it is the best inert coolant and will be similar to hydrogen due to its high specific heat, low molecular weight and high thermal conductivity. The latter is of interest because it is desirable to know if the injection of a good heat transfer medium gives an increase in convection heat transfer to the nozzle wall.

REFERENCES

1. Armour, W. H., et al, "An Investigation and Development of Film Protected-Convectively Cooled Nozzles," First Quarterly Report, Philco Research Laboratories, RPL-TDR-64-79, May 1964.

2. Carlson, D. J., et al, "Alumina Absorption and Emittance," Final Report, Philco Research Laboratories Publication No. U-2627, May 1964.

3. Price, F. C., et al, "Internal Environment of Solid Rocket Nozzle," Philco Research Laboratories Publication No. U-2709, August 1964.

4. Elliott, D. G., Bartz and Silver, S., "Calculation of Turbulent Boundary-Layer Growth and Heat Transfer in Axi-Symmetric Nozzles," TR No. 32-387, Jet Propulsion Laboratory, California Institute of Technology, February 15, 1963.

5. Hall, I. M., "Transonic Flow in Two-Dimensional and Axially-Symmetric Nozzles," Aeronautical Research Council, A.R.C. 23,347, 18 December 1961, also ASTIA AD 277 293.

6. Holt, N., "The Design of Plane and Axisymmetric Nozzles by the Method of Integral Relations," University of California, Institute of Engineering Research, Berkeley, California, Report No. 197, September 1962, also ASTIA AD 288 546.

7. Armour, W H., et al, "Applied Research for Advanced Cooled Nozzles (U)," Final Report, Philco Research Laboratories, RTD-TDR-63-1122, December 1963, Confidential.

U. S. Department of the Interior
Bureau of Mines
4800 Forbes Avenue
Pittsburgh 13, Pa

Attn: M. M. Dolinar
Repts Librarian
Explosives Research Lab
CP-3
1 Copy

Central Intelligence Agency
2430 E Street, N. W.
Washington 25, D. C.

Attn: OCD, Standard Dist
CP-6
1 Copy

Office of the Director of Defense
Research and Engineering
Washington 25, D. C.

Attn: D. B. Brooks
Office of Fuels and
Lubricants
CP-7
1 Copy

National Aeronautics and
Space Administration
Lewis Research Center
21000 Brookpark Road
Cleveland 35, Ohio

Attn: Library
CP-8
1 Copy

National Aeronautics and
Space Administration
Launch Operations Center
Cocoa Beach, Florida

Attn: Library
CP-9
1 Copy

National Aeronautics and
Space Administration
Manned Spacecraft Center
P. O. Box 1537
Houston 1, Texas

Attn: Library
CP-10
1 Copy

National Aeronautics and
Space Administration
George C. Marshall
Space Flight Center
Huntsville, Alabama

Attn: Library
CP-11
1 Copy

National Aeronautics and
Space Administration
Langley Research Center
Langley Air Force Base
Virginia

Attn: Library
CP-12
3 Copies

National Aeronautics and
Space Administration
Washington 25, D. C.

Attn: Office of Technical Information
and Educational Programs
Code ETL
CP-13
1 Copy

Scientific and Tech Info Facility
P. O. Box 5700
Bethesda, Maryland

Attn: NASA Representative
CP-14
2 Copies

National Aeronautics and
Space Administration
Washington 25, D. C.

Attn: R. W. Ziem (RPS) CP-209
1 Copy

National Aeronautics and
Space Administration
Goddard Space Flight Center
Greenbelt, Maryland

Attn: Library CP-210
1 Copy

Air Force Systems Command
Andrews AFB
Washington 25, D. C.

Attn: SCTAP CP-58
1 Copy

Arnold Eng Development Center
Air Force Systems Command
Tullahoma, Tennessee

Attn: AEOIM CP-59
1 Copy

Air Force Rocket Propulsion Lab
Edwards
California

Attn: DGPL CP-62
1 Copy

Air Force Rocket Propulsion Lab
Edwards
California

Attn: DGPS CP-63
1 Copy

Air Force Rocket Propulsion Lab
Edwards
California

Attn: DGR CP-64

Air Force Rocket Propulsion Lab
Edwards
California

Attn: DGS CP-65
1 Copy

Commander
Air Force Flight Test Center
Edwards AFB, California

Attn: Tech Library
Code FTBAT-2 CP-66
1 Copy

Air Force Missile Dev Center
Holloman AFB, New Mexico

Attn: MDGRT CP-69
1 Copy

Air Force Missile Test Center
Patrick Air Force Base
Florida

Attn: MTBAT CP-73
1 Copy

Commander
Aeronautical Research Laboratory
Wright-Patterson AFB, Ohio

Attn: AFC, Mr. Karl Scheller
CP-75
1 Copy

Aeronautical Systems Division
Wright-Patterson AFB, Ohio

Attn: ASRCEE-1 — CP-78, 1 Copy

Aeronautical Systems Division
Wright-Patterson AFB, Ohio

Attn: ASRCEM-1 — CP-79, 1 Copy

Commanding Officer
Ballistic Research Laboratories
Aberdeen Proving Ground, Maryland

Attn: BLI — CP-15, 1 Copy

Commanding Officer
Harry Diamond Laboratories
Washington 25, D. C.

Attn: AMXDO-TIB — CP-19, 1 Copy

Commanding Officer
Army Research Office (Durham)
Box CM, Duke Station
Durham, North Carolina
CP-21, 1 Copy

Commanding Officer
U. S. Army Chemical Research
and Development Laboratories
Edgewood Arsenal, Maryland

Attn: Chief, Physicochemical
Research Division
CP-22, 1 Copy

Commanding Officer
Picatinny Arsenal
Liquid Rocket Propulsion Lab
Dover, New Jersey

Attn: Technical Library
CP-26, 2 Copies

Commanding General
U. S. Army Missile Command
Redstone Arsenal, Alabama

Attn: Technical Library
CP-29, 5 Copies

Commanding General
White Sands Missile Range
New Mexico

Attn: Technical Library
CP-30, 1 Copy

Bureau of Naval Weapons
Department of the Navy
Washington 25, D. C.

Attn: DLI-3 — CP-34, 2 Copies

Bureau of Naval Weapons
Department of the Navy
Washington 25, D. C.

Attn: RMMP-2 — CP-35, 2 Copies

Bureau of Naval Weapons
Department of the Navy
Washington 25, D. C.

Attn: RMMP-3 — CP-36, 1 Copy

Bureau of Naval Weapons
Department of the Navy
Washington 25, D. C.

Attn: RMMP-4 — CP-37, 1 Copy

Bureau of Naval Weapons
Department of the Navy
Washington 25, D. C.

Attn: RRRE-6 — CP-38, 1 Copy

Commander
U. S. Naval Missile Center
Point Mugu, California

Attn: Technical Library — CP-40, 2 Copies

U. S. Naval Ordnance Laboratory
Corona, California

Attn: P. J. Slota, Jr. — CP-41, 1 Copy

Commander
U. S. Naval Ordnance Laboratory
White Oak
Silver Spring, Maryland

Attn: Library — CP-42, 2 Copies

Commander
U. S. Naval Ordnance Test Station
China Lake, California

Attn: Code 45 — CP-43, 5 Copies

Commander
U. S. Naval Ordnance Test Station
China Lake, California

Attn: Technical Library Branch — CP-44, 1 Copy

Superintendent
U. S. Naval Postgraduate School
Naval Academy
Monterey, California

CP-45, 1 Copy

Commanding Officer
U. S. Naval Propellant Plant
Indian Head, Maryland

Attn: Technical Library — CP-46, 2 Copies

Commanding Officer
Office of Naval Research
1030 E. Green Street
Pasadena 1, California

CP-51, 1 Copy

Director (Code 6180)
U. S. Naval Research Lab
Washington 25, D. C.

Attn: H. W. Carhart — CP-53, 1 Copy

Director
Special Projects Office
Department of the Navy
Washington 25, D. C.
CP-55
1 Copy

Commanding Officer
U. S. Naval Underwater
Ordnance Station
Newport, Rhode Island

Attn: W. W. Bartlett
CP-56
1 Copy

Commander
U. S. Naval Weapons Laboratory
Dahlgren, Virginia

Attn: Technical Library
CP-57
1 Copy

Aerojet-General Corporation
P. O. Box 296
Azusa, California

Attn: Librarian
CP-83
3 Copies

Aerojet-General Corporation
11711 South Woodruff Avenue
Downey, California

Attn: Florence Walsh
Librarian
CP-84
1 Copy

Aerojet-General Corporation
P. O. Box 1947
Sacramento, California

Attn: Technical Information Office
CP-85
3 Copies

Aeroprojects, Inc
310 East Rosedale Avenue
West Chester, Pennsylvania

Attn: C. D. McKinney
CP-87
1 Copy

Aerospace Corporation
P. O. Box 95085
Los Angeles 45, California

Attn: Library-Documents
CP-88
2 Copies

Allied Chemical Corporation
General Chemical Division
Research Lab
P. O. Box 405
Morristown, New Jersey

Attn: L. J. Wiltrakis
Security Officer
CP-91
1 Copy

Amcel Propulsion Company
Box 3049
Asheville, North Carolina
CP-92
1 Copy

American Cyanamid Company
1937 W. Main Street
Stamford, Connecticut

Attn: Security Officer
CP-93
1 Copy

Armour Research Foundation
of Illinois Institute of Technology
Technology Center
Chicago 16, Illinois

Attn: C. K. Hersh
Chemistry Division
CP-98
1 Copy

ARO, Inc
Arnold Engrg Dev Center
Arnold AF Station, Tennessee

Attn: Dr. B. H. Goethert
Director of Engrg
CP-99
1 Copy

Atlantic Research Corporation
Shirley Highway and Edsall Road
Alexandria, Virginia
CP-101
2 Copies

Atlantic Research Corporation
Western Division
209 Easy Street
El Monte, California

Attn: H. Niederman
CP-102
1 Copy

Battelle Memorial Institute
505 King Avenue
Columbus 1, Ohio

Attn: Report Library
Room 6A
CP-103
1 Copy

Bell Aerosystems
Box 1
Buffalo 5, New York

Attn: T. Reinhardt
CP-105
1 Copy

The Boeing Company
Aero Space Division
P. O. Box 3707
Seattle 24, Washington

Attn: R. R. Barber
Lib Ut Ch
CP-108
1 Copy

Chemical Propulsion Information
Agency
Applied Physics Laboratory
8621 Georgia Avenue
Silver Spring, Maryland
CP-114
3 Copies

Douglas Aircraft Co, Inc
Santa Monica Division
Santa Monica, California

Attn: Mr. J. L. Waisman
CP-122
1 Copy

The Dow Chemical Company
Security Section
Box 31
Midland, Michigan

Attn: Dr. R. S. Karpiuk
1710 Building
CP-123
1 Copy

E. I. duPont deNemours and Company
Eastern Laboratory
Gibbstown, New Jersey

Attn: Mrs. Alice R. Steward
CP-125
1 Copy

Esso Research and Engineering Co
Special Projects Unit
P. O. Box 8
Linden, New Jersey

Attn: Mr. D. L. Baeder
CP-126
1 Copy

Ethyl Corporation
Research Laboratories
1600 West Eight Mile Road
Ferndale, Michigan

Attn: E. B. Rifkin
Assistant Director
Chemical Research
CP-128
1 Copy

The Franklin Institute
20th and Parkway
Philadelphia 3, Pennsylvania

Attn: Miss Marion H. Johnson
Librarian
Technical Reports Library
CP-132
1 Copy

General Dynamics/Convair
San Diego 12, California

Attn: Engrg Library
K. G. Blair, Ch Librn
Mail Zone 50-03
CP-133
1 Copy

General Electric Company
Cincinnati 15, Ohio

Attn: Technical Information Agency
CP-134
1 Copy

Allison Division
General Motors Corporation
Indianapolis 6, Indiana

Attn: Plant 8, Tech Library
Mr. L. R. Smith
CP-135
1 Copy

Hercules Powder Company
Allegany Ballistics Laboratory
P. O. Box 210
Cumberland, Maryland

Attn: Library
CP-138
3 Copies

Hercules Powder Company
Kenvil
New Jersey

Attn: Library
CP-139
1 Copy

Hercules Powder Company
Research Center
Wilmington 99, Delaware

Attn: Dr. Herman Skolnik
Manager Tech Info Div
CP-142
1 Copy

Institute for Defense Analysis
Res and Eng Support Division
1825 Connecticut Avenue
Washington 9, D. C.

Attn: Technical Information Office
CP-146
1 Copy

Jet Propulsion Laboratory
4800 Oak Grove Drive
Pasadena 3, California

Attn: L. E. Newlan
Chief, Reports Group
CP-147
1 Copy

Lockheed Propulsion Company
P. O. Box 111
Redlands, California

Attn: Miss Belle Berlad
Librarian CP-152
3 Copies

Marquardt Corp
16555 Saticoy Street
Box 2013 - South Annex
Van Nuys, California
CP-155
1 Copy

Minnesota Mining and
Manufacturing Co
900 Bush Avenue
St. Paul 6, Minnesota

Attn: J. D. Ross

VIA: H. C. Zeman
Security Administrator
CP-159
2 Copies

Monsanto Research Corporation
Boston Labs, Everett Station
Boston 49, Massachusetts

Attn: Library CP-161
1 Copy

New York University
Research Building No. 3
233 Fordham Landing Road
University Heights 68, New York

Attn: Document Control - CJM
CP-164
1 Copy

New York University
Dept of Chemical Engineering
New York 53, New York

Attn: P. F. Winternitz
CP-165
1 Copy

North American Aviation, Inc
Space and Information Systems Div
12214 Lakewood Boulevard
Downey, California

Attn: W. H. Morita CP-166
1 Copy

Purdue University
Lafayette, Indiana

Attn: M. J. Zucrow CP-174
1 Copy

Rocketdyne
6633 Canoga Avenue
Canoga Park, California

Attn: Library, Dept 596-306
CP-180
3 Copies

Rohm and Haas Company
Redstone Arsenal Research Division
Huntsville, Alabama

Attn: Librarian — CP-182, 2 Copies

Space Technology Laboratory, Inc
1 Space Park
Redondo Beach, California

Attn: STL Tech Lib Doc Acquisitions — CP-185, 2 Copies

Texaco Experiment Incorporated
P. O. Box 1-T
Richmond 2, Virginia

Attn: Librarian — CP-187, 1 Copy

Thiokol Chemical Corporation
Alpha Division, Huntsville Plant
Huntsville, Alabama

Attn: Technical Director — CP-189, 2 Copies

Thiokol Chemical Corporation
Alpha Division
Space Booster Plant
Brunswick, Georgia

CP-190, 1 Copy

Thiokol Chemical Corporation
Elkton Division
Elkton, Maryland

Attn: Librarian — CP-192, 1 Copy

Thiokol Chemical Corporation
Reaction Motors Division
Denville, New Jersey

Attn: Librarian — CP-193, 1 Copy

Thiokol Chemical Corporation
Rocket Operations Center
P. O. Box 1640
Ogden, Utah

Attn: Librarian — CP-194, 1 Copy

Thiokol Chemical Corporation
Wasatch Division
P. O. Box 524
Brigham City, Utah

Attn: Library Section — CP-195, 2 Copies

Thompson Ramo-Wooldridge
23555 Euclid Avenue
Cleveland 17, Ohio

Attn: Librarian — CP-196, 2 Copies

Union Carbide Chemicals Co
P. O. Box 8584 (Technical Center)
South Charleston 3, West Virginia

Attn: Dr. H. W. Schulz — CP-197, 1 Copy

United Aircraft Corporation
Corporation Library
400 Main Street
East Hartford, Connecticut

Attn: Dr. David Rix — CP-201, 1 Copy

United Aircraft Corporation
Pratt and Whitney Fla Res
and Dev Ctr
P. O. Box 2691
W. Palm Beach, Florida

Attn: Library — CP-202, 1 Copy

United Technology Center
P. O. Box 358
Sunnyvale, California

Attn: Librarian — CP-204, 1 Copy

British Defence Staff
British Embassy
3100 Massachusetts Avenue
Washington, D. C.

Attn: Scientific Information Officer — F-1, 4 Copies

VIA: Headquarters
Air Force Ssystems Command
Andrews Air Force Base
Washington 25, D. C.

Attn: SCS-41(3-1833)

Defence Research Member
Canadian Joint Staff (W)
2450 Massachusetts Avenue
Washington, D. C.

VIA: Headquarters
Air Force Systems Command
Andrews Air Force Base
Washington 25, D. C.

Attn: SCS-41 (3-1833) — F-2, 4 Copies

Defense Documentation Center
Cameron Station, Bldg 5,
Alexandria, Virginia — CP-61, 20 Copies

American Machine and Foundry Co
Mechanics Research Department
7501 North Natchez Avenue
Niles 48, Illinois

Attn: Phil Rosenberg — CP-94, 1 Copy

Callery Chemical Company
Research and Development
Callery, Pennsylvania

Attn: Document Control — CP-111, 1 Copy

B. F. Goodrich Aerospace
and Defense Products
P. O. Box 157
Rialto, California

Attn: Mr. A. B. Japs
Tech Manager
Rocket Motor Development — CP-136, 1 Copy

Hercules Powder Company
Bacchus Works
Magna, Utah

Attn: Librarian — CP-140
1 Copy

Hynes Research Corporation
308 Bon Air Avenue
Durham, North Carolina

CP-144
1 Copy

Walter Kidde Company
675 Main Street
Belleville 9, New Jersey

Attn: Security Librarian

CP-148
1 Copy

Olin Mathieson Chemical Corp
Marion, Illinois

Attn: Research Library
Box 508 — CP-168
1 Copy

Olin Mathieson Chemical Corp
Research Library 1-K-3
275 Winchester Avenue
New Haven, Connecticut

Attn: Mail Control Room
Miss Laura M. Kajuti

CP-169
1 Copy

Pennsalt Chemicals Corporation
900 First Avenue
King of Prussia, Pennsylvania 19406

Attn: Mr. W. M. Lee — CP-170
1 Copy

Phillips Petroleum Company
145 Chemical Labs Bldg
Bartlesville, Oklahoma

Attn: H. M. Fox — CP-172
1 Copy

Rocketdyne, A Division of
North American Aviation, Inc.
Solid Propulsion Operations
P. O. Box 548
McGregor, Texas

Attn: Library — CP-181
1 Copy

Wright Aeronautical Division
Curtiss-Wright Corporation
Wood-Ridge, New Jersey

CP-207
1 Copy

ARDE-Portland, Inc.
Research and Development Office
100 West Century Road
Paramus, New Jersey

Attn: Library — CP-97
1 Copy

The Carborundum Company
Box Number 162
Niagara Falls, New York — CP-112
1 Copy

Chemical Research and
Development Center
FMC Corporation
P. O. Box 8
Princeton, New Jersey

Attn: Security Officer — CP-115
1 Copy

Union Carbide Corporation
270 Park Avenue
New York 17, New York

Attn: B. J. Miller — CP-200
1 Copy

Aeronautical Systems Division
Wright-Patterson AFB, Ohio

Attn: ASRCMC — 1 Copy